

UNCLASSIFIED

AD NUMBER
ADB223904
NEW LIMITATION CHANGE
TO Approved for public release, distribution unlimited
FROM Distribution authorized to U.S. Gov't. agencies only; Proprietary Info; Dec 96. Other requests shall be referred to Commander, U.S. Army Medical Research and Materiel Command, ATTN: MCMR-RMI-S, Fort Detrick, Frederick, MD 21702-5012.
AUTHORITY
P. M. Rinehart, Deputy Chief of Staff for Info. Mgmt., USAMRMC, MCMR-RMI-S [70-1y], Ft. Detrick, MD.

THIS PAGE IS UNCLASSIFIED

AD _____

MIPR NUMBER 93MM3571

TITLE: The Cytoskeleton & ATP in Sulfur Mustard-Mediated Injury
to Endothelial Cells & Keratinocytes

PRINCIPAL INVESTIGATOR: Daniel B. Hinshaw, M.D.

CONTRACTING ORGANIZATION: Ann Arbor Veterans Administration
Medical Center
Ann Arbor, Michigan 48105

REPORT DATE: December 1996

TYPE OF REPORT: Final

PREPARED FOR: Commander
U.S. Army Medical Research and Materiel Command
Fort Detrick, Frederick, Maryland 21702-5012

DISTRIBUTION STATEMENT: Distribution authorized to U.S. Government
agencies only (proprietary information, Dec 96). Other requests
for this document shall be referred to Commander, U.S. Army Medical
Research and Materiel Command, ATTN: MCMR-RMI-S, Fort Detrick,
Frederick, MD 21702-5012.

The views, opinions and/or findings contained in this report are those
of the author(s) and should not be construed as an official Department
of the Army position, policy or decision unless so designated by other
documentation.

19970516 052

REPORT DOCUMENTATION PAGE

Form Approved
OMB No. 0704-0188

Public reporting burden for this collection of information is estimated to average 1 hour per response, including the time for reviewing instructions, searching existing data sources, gathering and maintaining the data needed, and completing and reviewing the collection of information. Send comments regarding this burden estimate or any other aspect of this collection of information, including suggestions for reducing this burden, to Washington Headquarters Services, Directorate for Information Operations and Reports, 1215 Jefferson Davis Highway, Suite 1204, Arlington, VA 22202-4302, and to the Office of Management and Budget, Paperwork Reduction Project (0704-0188), Washington, DC 20503.

1. AGENCY USE ONLY (Leave blank)		2. REPORT DATE December 1996		3. REPORT TYPE AND DATES COVERED Final (1 Jul 93 - 30 Sep 96)	
4. TITLE AND SUBTITLE The Cytoskeleton & ATP in Sulfur Mustard-Mediated Injury to Endothelial Cells & Keratinocytes				5. FUNDING NUMBERS MIPR 93MM3571	
6. AUTHOR(S) Daniel B. Hinshaw, M.D.					
7. PERFORMING ORGANIZATION NAME(S) AND ADDRESS(ES) Ann Arbor Veterans Administration Medical Center Ann Arbor, Michigan 48105				8. PERFORMING ORGANIZATION REPORT NUMBER	
9. SPONSORING/MONITORING AGENCY NAME(S) AND ADDRESS(ES) U.S. Army Medical Research and Materiel Command Fort Detrick Frederick, Maryland 21702-5012				10. SPONSORING/MONITORING AGENCY REPORT NUMBER	
11. SUPPLEMENTARY NOTES					
12a. DISTRIBUTION / AVAILABILITY STATEMENT Distribution authorized to U.S. Government agencies only (proprietary information, Dec 96). Other requests for this document shall be referred to Commander, U.S. Army Medical Research and Materiel Command, ATTN: MCMR-RMI-S, Fort Detrick, Frederick, MD 21702-5012.				12b. DISTRIBUTION CODE	
13. ABSTRACT (Maximum 200) The goal of this project has been to define the nature of the cytopathology induced by sulfur mustard (SM) in endothelial cells and keratinocytes which accounts for vesication. Using fluorescence microscopic techniques and biochemical assays we tested the hypotheses that SM injury can cause two forms of cell death in endothelial cells and keratinocytes, apoptosis and necrosis, and that they result in cytoskeletal and morphologic changes which account for SM-induced blister formation. SM induced apoptosis and necrosis in endothelial cells, but only caused necrosis in keratinocytes. Minimal cell death was seen in keratinocytes with $\leq 250 \mu\text{M}$ SM, which did cause apoptosis in endothelial cells. Actin filament disassembly or depolymerization was a common feature of injury in both cell types. SM-mediated alterations in microfilament organization and cellular shape correlated well with loss of cellular adherence and endothelial permeability barrier function. SM caused reductions in ATP and NAD ⁺ in both cell types, but was associated with increased poly-(ADP-ribose)-polymerase activity only in endothelial cells. Polyacrylamide gel electrophoretic-analysis of cytoskeletal extracts under non-reducing conditions and measurements of glutathione provided evidence for an oxidative challenge during SM injury in keratinocytes. Thus, SM induces two very different patterns of cell injury in keratinocytes and endothelial cells. Cytoskeletal pathology common to both patterns of injury may be critical to the pathogenesis of vesication.					
14. SUBJECT TERMS Sulfur, Mustard, CD Microfilaments, Apoptosis, Necrosis, Cell Death, Sulfur Mustard				15. NUMBER OF PAGES 45	
				16. PRICE CODE	
17. SECURITY CLASSIFICATION OF REPORT Unclassified	18. SECURITY CLASSIFICATION OF THIS PAGE Unclassified	19. SECURITY CLASSIFICATION OF ABSTRACT Unclassified	20. LIMITATION OF ABSTRACT Limited		

FOREWORD

Opinions, interpretations, conclusions and recommendations are those of the author and are not necessarily endorsed by the U.S. Army.

DSM Where copyrighted material is quoted, permission has been obtained to use such material.

DSM Where material from documents designated for limited distribution is quoted, permission has been obtained to use the material.

DSM Citations of commercial organizations and trade names in this report do not constitute an official Department of Army endorsement or approval of the products or services of these organizations.

NIA In conducting research using animals, the investigator(s) adhered to the "Guide for the Care and Use of Laboratory Animals," prepared by the Committee on Care and use of Laboratory Animals of the Institute of Laboratory Resources, national Research Council (NIH Publication No. 86-23, Revised 1985).

DSM For the protection of human subjects, the investigator(s) adhered to policies of applicable Federal Law 45 CFR 46.

NIA In conducting research utilizing recombinant DNA technology, the investigator(s) adhered to current guidelines promulgated by the National Institutes of Health.

NIA In the conduct of research utilizing recombinant DNA, the investigator(s) adhered to the NIH Guidelines for Research Involving Recombinant DNA Molecules.

NIA In the conduct of research involving hazardous organisms, the investigator(s) adhered to the CDC-NIH Guide for Biosafety in Microbiological and Biomedical Laboratories.

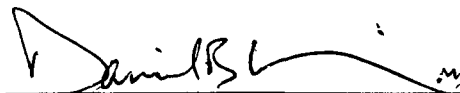
 12/23/96
PI - Signature Date

TABLE OF CONTENTS

Front Cover	Page 1
SF 298 - Report Documentation Page	Page 2
Foreword	Page 3
Table of Contents	Page 4
Introduction	Pages 5 through 8
Body	Pages 8 through 40
Conclusions	Pages 40 through 42
References	Pages 43 through 44
Bibliography (Publications, Abstracts)	Page 45
Personnel	Page 45

*Denotes pages which contain proprietary or unpublished data.

DTIC QUALITY INSPECTED 3

INTRODUCTION

Although it has been seventy eight years since the cessation of hostilities in World War I in which the chemical warfare vesicating agent, sulfur mustard (SM), was introduced, there is still no effective means of treating the devastating effects of this weapon of terror. Effective therapy will depend upon a thorough understanding of pathogenetic mechanisms. The primary goal of this project has been to examine the nature of the pathologic changes (including cell death) induced in endothelial cells and keratinocytes by SM which may lead to blister formation.

Endothelial cells and keratinocytes are major cellular targets damaged early during the development of SM-induced vesication (1,2). Capillary leak resulting in rapid accumulation of local edema and blister fluid may not so much depend on endothelial cell death as upon altered endothelial morphology and adherence characteristics (1). Ultrastructural examination following SM injury has revealed membrane blebbing and damage to filaments of hemidesmosomes which normally anchor basal keratinocytes to the basal lamina (3). Changes in endothelial and keratinocyte morphology and adherence after SM exposure may be due to altered integrity of the cytoskeleton, the major structural determinant of cellular architecture and shape. Altered cytoskeletal organization and function in endothelial cells and keratinocytes after SM injury may thus account for both the loss of keratinocyte adherence to its basal lamina and the capillary leak secondary to endothelial cell dysfunction which lead to blister formation.

The cytoskeleton in most cells consists of three major structures: microfilaments, microtubules and intermediate filaments. Microfilaments which contain a backbone of polymerized or filamentous (F)-actin appear to play a dominant role in regulating cellular adherence to other cells and to the underlying substrate, thus influencing directly the integrity of cellular monolayers. Until recently, the actin present within the insoluble residue after cellular extraction with detergents like Triton X-100 (Tx-100) was felt to

include all of the F-actin present in the cell (4). However, recent studies with neutrophils have demonstrated that in addition to the detergent-insoluble or stable pool of F-actin there may also be a labile pool of F-actin present within cells (5) which is detergent-soluble (6). Removal of chemoattractant ligands from the lamellipodia of chemotaxing neutrophils has been noted to cause rapid depolymerization of actin filaments only in the lamellipodia of the cells (5). The depolymerization of these "labile" actin filaments has been closely correlated with transient blebbing of the overlying surface of the cells (5). We have shown recently that detergent (Tx-100)-insoluble-(stable) and Tx-100-soluble (labile) pools of F-actin are also present in adherent endothelial cells (7).

Cell death usually results from one of two processes: 1) necrosis, a pathologic form of death occurring as a result of injury or 2) apoptosis (8-10). Injury leading to necrosis is typically associated with cellular swelling and loss of plasma membrane integrity.

Apoptosis is the form of cell death characterized by a morphologic pattern of nuclear fragmentation and condensation associated with cell shrinkage ultimately leading to fragmentation of the cell into many smaller membrane enclosed fragments (apoptotic bodies) which contain portions of the fragmented chromatin. The apoptotic bodies retain intact plasma membranes for some time and *in vivo* are phagocytized by neighboring cells (8-10). Whereas the cell lysis of necrosis is usually associated with an acute inflammatory response, apoptotic death typically occurs "silently" without acute inflammation (8).

The pattern of cell death in terms of kinetics and dose response reported for SM (11,12) suggests that this toxic agent may also induce the slower apoptotic death at lower concentrations and the more rapid necrotic death at higher concentrations which has been reported for other toxic agents (8). This implies that the "suicide" program of apoptosis might be initiated by SM exposure, but at higher concentrations of the agent other direct toxic effects of the agent (e.g. on cellular metabolism) may cause the necrotic form of cell death to supervene with resultant cell lysis prior to full expression of the apoptotic phenotype.

In work reviewed in the midterm report for this project, the role of microfilaments in coordinating the morphologic events of apoptosis was characterized (13). Briefly, using flow cytometry, polyacrylamide gel electrophoresis, and fluorescence microscopy, we showed that apoptosis induced by ultraviolet (UV) irradiation or 80 $\mu\text{g/ml}$ etoposide correlates with early transient polymerization and later depolymerization of filamentous (F)-actin and dramatic changes in visible microfilament organization. Depolymerization of F-actin began before the formation of apoptotic bodies and was ultimately composed of decreases in both the detergent-insoluble (40%) and detergent-soluble (50%) pools of F-actin. Dihydrocytochalasin B (H_2CB), which blocked apoptotic body formation, depolymerized F-actin in the detergent-insoluble pool only. Visually, H_2CB treatment disrupted microfilament organization, resulting in short, brightly stained microfilaments dispersed throughout the cytoplasm. In contrast, apoptotic cells contained a network of fine microfilaments with bright staining concentrated at the site of the apoptotic body formation. Together, these results suggested that reorganization of the microfilament network is necessary for the formation of apoptotic bodies and that depolymerization of F-actin may also be a necessary component of the process of apoptosis.

In a model of endothelial cell injury (also reviewed in the midterm report) induced by the oxidant hydrogen peroxide, H_2O_2 , we found that apoptosis is ATP-dependent and that the amino acid glutamine can be utilized by oxidant-injured endothelial cells to generate sufficient ATP to convert necrosis to apoptosis (14).

Other studies addressing the SOW of this project (reviewed in detail in the midterm report) examined the nature of endothelial cell death induced by SM (15). To summarize these findings: endothelial cells were exposed to 0 - 1000 μM SM over the time course of 2 - 24 hr to determine the role of apoptotic and necrotic patterns of cell death in endothelial injury induced by SM. SM concentrations ≤ 250 μM induced exclusively apoptosis which was observed after 5 hr in 30% of endothelial cells. Exposure to SM concentrations ≥ 500 μM caused apoptosis and necrosis to the same extent in 60 - 85% of all cells after 5 to 6 hr.

Necrosis was accompanied by a significant (~50%) depletion of intracellular ATP, while in apoptotic cells ATP remained at the level similar to healthy cells. Interestingly, disruption of the long actin filament stress fibers and rounding of cells preceded other features of apoptosis — DNA fragmentation, membrane budding, and apoptotic body formation. In apoptotic cells, microfilaments formed constricted perinuclear bands, which were not observed in necrotic cells. Pretreatment with 50 mM N-acetyl-L-cysteine (NAC), a sulfhydryl donor and antioxidant (16), nearly eliminated the apoptotic features of cell death but did not prevent necrosis in response to SM. NAC pretreatment alone induced reorganization of actin filaments into an enhanced network of long stress fibers transversing the length and width of the cells instead of a single dominant peripheral (cortical) band or ring of actin filaments. NAC pretreatment prevented loss of cell adherence and cell rounding following exposure to 250 μ M SM. The effect of NAC on cytoskeletal organization and its ability to eliminate SM-induced apoptosis suggests that actin filament organization may be an important element in cellular susceptibility to apoptotic stimuli.

In the body of this report we will review the remaining portions of the work addressing the SOW which will provide interesting insights into the different ways endothelial cells and keratinocytes respond to SM injury.

BODY

METHODS.

Cells and culture. Bovine pulmonary artery endothelial cells were purchased from the National Institute of Aging, Aging Cell Culture Repository (Camden, NJ) and maintained in RPMI 1640 medium supplemented with 2 mM glutamine (GIBCO), 10% heat-inactivated fetal bovine serum (Whitaker, M.A. Bioproducts), 10 mM HEPES, 100 U/ml penicillin, and 100 mg/ml streptomycin (GIBCO). Endothelial subculturing was carried out on confluent cultures using 0.05% trypsin and 0.02% EDTA (Sigma) and cells

of Passages 3 to 7 were used. Human keratinocytes from redundant skin removed at the time of reduction mammoplasty (courtesy of Dr. Cynthia Marcelo, University of Michigan) were grown in keratinocyte-SFM (GIBCO) to which 25 µg/ml bovine pituitary extract, 0.2 ng/ml epidermal growth factor and 5 µg/ml gentamicin were added. Upon reaching 80% confluence, the keratinocytes were passaged by exposure to 0.05% trypsin and 0.02% EDTA. The trypsin was inactivated with 10-15 ml of 0.3 mg/ml soybean trypsin inhibitor (Sigma). Keratinocytes from the first to third passages were used for experiments. Cells were grown in 75- or 150-cm² flasks (Falcon) in a culture incubator at 37°C under a 5% CO₂ humidified atmosphere.

Injury protocol with SM. Confluent monolayers of endothelial cells or keratinocytes grown in six-well plates (Falcon, Becton Dickinson) were exposed to final concentrations of SM ranging from 0.1 to 1 mM in culture media under sterile conditions. Biochemical and morphological parameters of SM injury were monitored at multiple time points. Matched controls were also done over identical conditions and time points to which no SM had been added.

In the experiments in which cells were pretreated with N-acetyl-cysteine (NAC) to block apoptosis (16), the cells were incubated for 20 hours with 50 mM N-acetyl-L-cysteine (Sigma) (16). Residual NAC in the media was removed by three washings with media before SM addition.

Cell morphology. Microscopic observations of endothelial cells and keratinocytes were performed during the time course of SM injury with a Nikon optiphot microscope. Wright-Giemsa staining was performed using the Fisher LeukoStat Stain Kit.

Determination of apoptotic index and cell viability (17). Adherent cells grown in six-well plates were stained during the time course of SM injury with a dye mixture (10 μ M acridine orange and 10 μ M ethidium bromide; (Sigma), that was prepared in phosphate-buffered saline (PBS)).

Acridine orange (fluorescent DNA-binding) intercalates into DNA, making it appear green, and binds to RNA, staining it red-orange. Ethidium bromide is taken up only by nonviable cells, and its fluorescence overwhelms that of the acridine orange, making the chromatin of lysed cells appear orange.

At the end of each experimental time point, all of the medium was removed and cells were harvested by incubation with 0.05% trypsin and 0.02% EDTA for 1 min and washed with the medium. Then, 250 μ l of cell suspension was mixed with 10 μ l of the dye mix and 200 cells per sample were examined by fluorescence microscopy, according to the following criteria: (1) viable cells with normal nuclei (fine reticular pattern of green stain in the nucleus and red-orange granules in the cytoplasm); (2) viable cells with apoptotic nuclei (green chromatin which is highly condensed or fragmented and uniformly stained by the acridine orange); (3) nonviable cells with normal nuclei (bright orange chromatin with organized structure); and (4) nonviable cells with apoptotic nuclei (bright orange chromatin which is highly condensed or fragmented).

The study of the viability of cells in the undisturbed monolayers has shown that trypsinization does not promote further cell injury.

ATP measurement. Cellular ATP levels were assayed as previously reported by the luciferase-luciferin method of Stanley and Williams (15). The luciferase-luciferin (Sigma) was reconstituted in a buffer containing 1% bovine serum albumin, 20 mM

glycine, and 2 mM EDTA, pH 8.0. Measurements were performed in an LKB Model 1251 automated luminometer (LKB Instruments, Inc., Gaithersburg, MD). ATP data were expressed as nanomoles of ATP per 1×10^6 cells. The whole cell population, including any floating cells, was subjected to the assay.

In some experiments in which the effect of glutamine supplementation on ATP levels was examined, 1×10^6 keratinocytes or endothelial cells/well were grown in 12-well plates. After two days the cells were washed three times with L-glutamine free medium and incubated in this medium for 1 hr. After the incubation, 0, 2 or 4 mM of L-glutamine was added. After 1 hr, the cells were injured with 0, 250, 500 or 1000 μ M SM. Five hours after the injury, ATP was measured using the luciferin-luciferase method (15). The keratinocytes did not tolerate long (20-24 hr) periods of glutamine deprivation, during which a majority of the cells died (data not shown), thus necessitating the shorter period of glutamine deprivation.

DNase I assay. The DNase I assay was used as previously described (7) for measurement of actin polymerization with the following modifications for adherent cells: cells grown to confluence in six-well plates were exposed to SM for variable periods of time. At the end of each experimental incubation, all of the medium in each well was removed and 1 ml of lysate solution containing 2 mM MgCl_2 , 2 mM EGTA, 0.2 mM ATP, 0.5 mM dithiothreitol, 3% Triton X-100 (Tx-100), and 1 mM phenylmethylsulfonyl fluoride (PMSF) in Hanks' buffered salt solution was added to each well and pipetted 5 or 6 times to release all of the cells. Floating cells were also subjected to the assay. This was either immediately assayed for G-actin or added to an equal aliquot of a solution containing 1.5 M guanidine HCl, 1 M NaCH_2CO_2 , 1 mM CaCl_2 , 1 mM ATP, and 20 mM Tris-HCl, pH 7.5, mixed, and placed on ice for 20 min for later assay of total actin using the published method (7).

Fluorescence microscopy. After varying periods of incubation at 37°C under the different experimental conditions, the adherent cells were fixed with 2% paraformaldehyde for 1 hr at room temperature. The paraformaldehyde was then removed and the cells were washed and permeabilized three times for 5 min with Dulbecco's Cation Free PBS, pH 7.4, containing 0.2% Triton X-100. Cells were either stained with 165 nM rhodamine phalloidin (Molecular Probes) specific for F-actin in microfilaments (18) for 20 min at room temperature in the dark or exposed to a 1:50 dilution of antibody to tubulin within microtubules (1 mg/ml monoclonal mouse anti- β tubulin (Boehringer, Mannheim)) or to a 1:20 dilution of antibody to cytokeratin (monoclonal anti-pan cytokeratin, Sigma Immunochemicals) and then reacted with a rhodamine-conjugated anti-IgG to achieve visualization of the stained structures. Coverslips were sealed to each monolayer and the samples were viewed with the G filter block on a Nikon optiphot fluorescence microscope. Fluorescence micrographs were taken using TMAX 400 film (Kodak).

NAD Assay (19). At different time points after sulfur mustard injury, cells were trypsinized and pellets were washed with cold PBS and resuspended in 0.2 ml of 0.5 M perchloric acid. After 15 min on ice, the cell extracts were neutralized with an equal volume of 1 M KOH, 0.33 M KH_2PO_4 - K_2HPO_4 (pH 7.5). After 15 min on ice, the insoluble KClO_4 was removed by centrifugation at 12,000 RPM for 5 min. The final supernatants were frozen until used for NAD measurements. NAD was measured as described by Jacobson and Jacobson (19). Briefly, 1 ml of NAD reaction mixture (600 mM ethanol, 0.5 mM 3-[4, 5 dimethylthiazol-2-yl]-2,5 diphenyltetrazolium bromide (MTT), 2 mM phenazine ethosulfate, 5 mM EDTA, 1 mg/ml BSA, 120 mM bicine, pH 7.8) was added to 0.2 ml of a cell extract or NAD standard (15-240 pmoles). The tubes were incubated at 37°C in the dark for 5 min and then 0.1 ml alcohol dehydrogenase (0.5 mg/ml in 100 mM bicine, pH 7.8) was added. After mixing, the samples were further

incubated for 20 min at 37°C. The reaction was stopped by adding 0.5 ml of 12 mM iodoacetate. The optical densities were measured spectrophotometrically at 570 nm, and data were expressed as pmole NAD⁺/mg protein.

Determination of poly-ADP-ribose-polymerase activity (20). Adherent cells in six-well plates were washed with media at various intervals after SM exposure and then exposed to 56 mM HEPES buffer, pH 7.5, containing 28 mM KCl, 28 mM NaCl, 2 mM MgCl₂, 0.01% digitonin, and 125 nmol NAD spiked with 0.25 μ Ci ³H-NAD (ICN Biomedicals, Costa Mesa, CA). The amount of digitonin used (21) permeabilizes plasma membranes leading to release of cytoplasmic enzymes, but not to loss of intracellular organelles. The permeabilized cells are incubated for 5 min at 37°C and the ADP-ribosylated protein was precipitated with 200 μ L 50% TCA. After two washes with TCA, the protein pellet was solubilized in 2% SDS in 0.1 M NaOH, incubated at 37°C overnight, and the radioactivity was determined by scintillation counting.

Glutathione Measurements. Total glutathione (GSH) and oxidized glutathione (GSSG) were measured using standard methods (22,23). Briefly, 5×10^6 cells were centrifuged for 30 s in a microcentrifuge, the supernatant removed and the pellet deproteinized with 200 μ L 2.5% sulfosalicylic acid in 0.2% Triton x-100. After another centrifugation, 100 μ L of supernatant was incubated with 2 μ L 2-vinylpyridine in 10 μ L of 1 M Tris base for 50 min at room temperature for the determination of GSSG. Total GSH and GSSG were determined in plastic cuvettes using 25- μ L samples for total GSH and 50 μ L samples for GSSG after addition of 500 μ L 0.3 mM 5,5' dithiobis 2-nitrobenzoic acid (DTNB), 500 μ L 0.4 mM NADPH containing 0.12 U glutathione reductase and 500 μ L phosphate/imidazole buffer, pH 7.2. The difference in optical density at 412 nm was read on a spectrophotometer.

SDS-Page Analysis of NAC Pretreated Cells Exposed to Sulfur

Mustard. Keratinocytes or BECs were pretreated with plus or minus 50 mM N-acetyl/cysteine (NAC) for 24 hr and then injured with 0, 250, and 1,000 μ M SM. Five hours after the injury, the cells were trypsinized and centrifuged. The pellets were resuspended in 400 μ l of lysis buffer (10 mM imidazole, 40 mM KCl, 10 mM EGTA, 1% triton X-100, pH 7.5) containing 1 mM PMSF, 10 μ g/ml aprotinin, and 10 μ g/ml leupeptin. After 5 min at room temperature, the samples were centrifuged at 12,000 RPM for 5 min. To the pellets (triton-insoluble material), 120 μ l of 1X sample buffer was added. The samples were sonicated and centrifuged. Protein determinations were made using the DC Protein Assay kit (Bio-Rad).

The triton-soluble material containing small actin filaments and monomeric (G)-actin (supernatants from the cell lysis) was transferred to new tubes and precipitated with 60 μ l of 80% TCA. After 1.5 hr, the samples were centrifuged and the pellets were washed twice with acetone. After evaporating the acetone, 240 μ l of sample buffer and 10 μ l of saturated tris base were added to the pellets. The samples were sonicated, centrifuged and amount of protein was determined.

Triton-soluble and -insoluble pools were equally divided. To half of each pool, 5% β -mercaptoethanol was added. All samples were boiled for 5 min and run on 12% sodium dodecyl sulfate (SDS) polyacrylamide gels.

Relative optical density of the bands (e.g. actin) was measured with a microcomputer imaging device that contains image analysis software (Imaging Research, Brock University, Ontario, Canada). Data are expressed as percent change from control band content (control = 100%), assuming relative optical density is directly proportional to protein content.

Measurement of Keratinocyte Adherence (15). Keratinocytes cultured in 6-well plates were washed twice with fresh SFM keratinocyte medium to remove dead (floating cells). The adherent cells were then treated with 0, 250, 500 or 1,000 μM SM. At 3, 5 and 6 hrs after the injury, adherence was determined by washing the cells twice with fresh medium and counting them after harvesting with 0.05% trypsin and 0.02% EDTA. The data were expressed as a percentage of cell number at time zero.

Endothelial Permeability Assay (24). 2×10^6 bovine endothelial cells/well were plated in Corning Transwell plates (3.0 μm pore size, 24 mm diameter). After 3-4 days of growth, the cells were exposed to 0, 250, 500 or 1,000 μM SM. After 3.5 hr of injury, the old media was removed and 2 ml of fresh RPMI (without phenol red) was added to the bottom chambers. To the plate inserts, 1.5 ml of the RPMI plus 1% albumin was added. After 0.5 hr and 1 hr, 100 μl was removed from the bottom chambers and mixed with 1 ml of albumin reagent (0.3 mmol/L bromocresol green). The absorbance, which was proportional to albumin content, was measured at 628 nm on a spectrophotometer. Data were expressed as a percentage of the absorbance of 100 μl of 1% albumin (i.e., conditions equal to the albumin concentration in the upper chamber at the beginning of the assay).

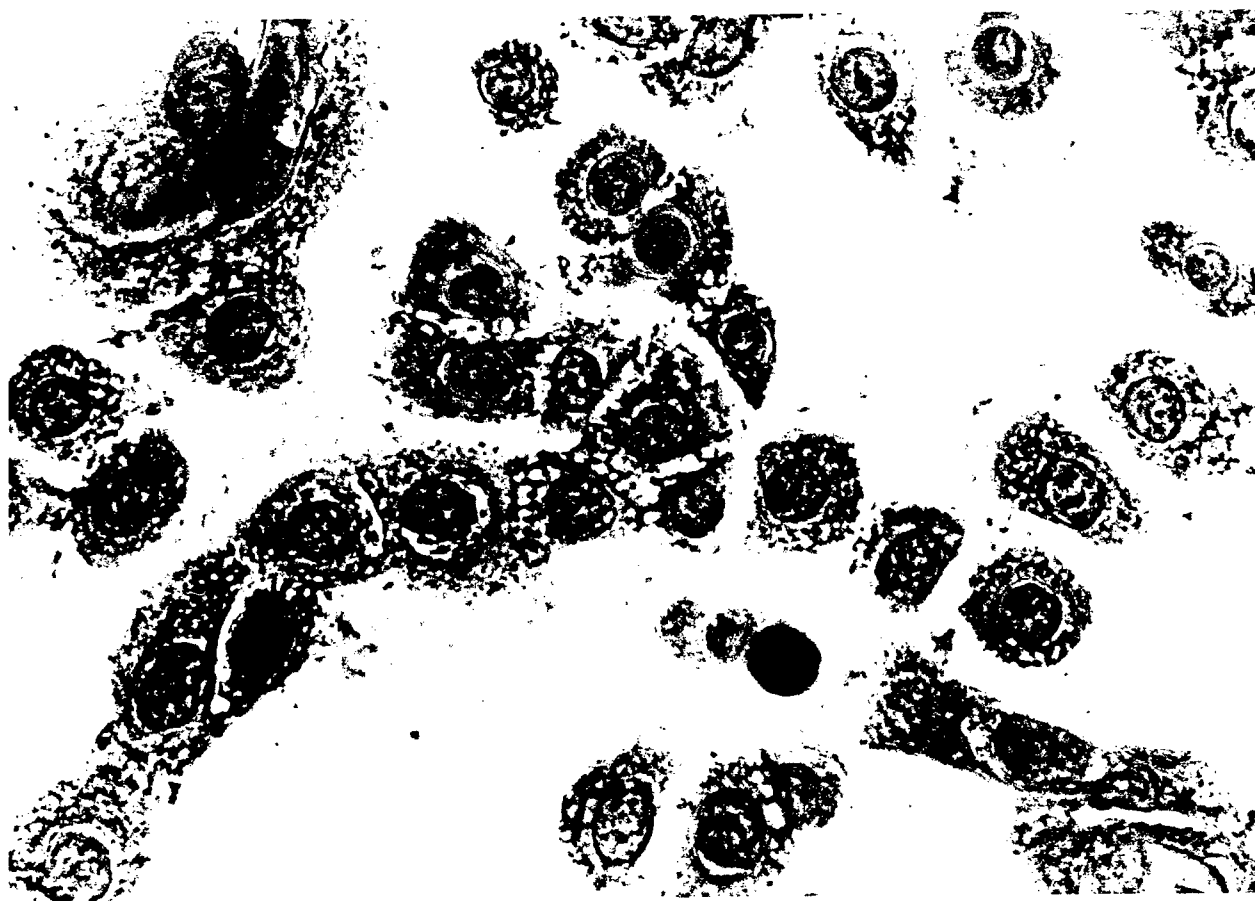
RESULTS

SM injury of keratinocytes - effect of SM on morphology, cytoskeleton, and viability

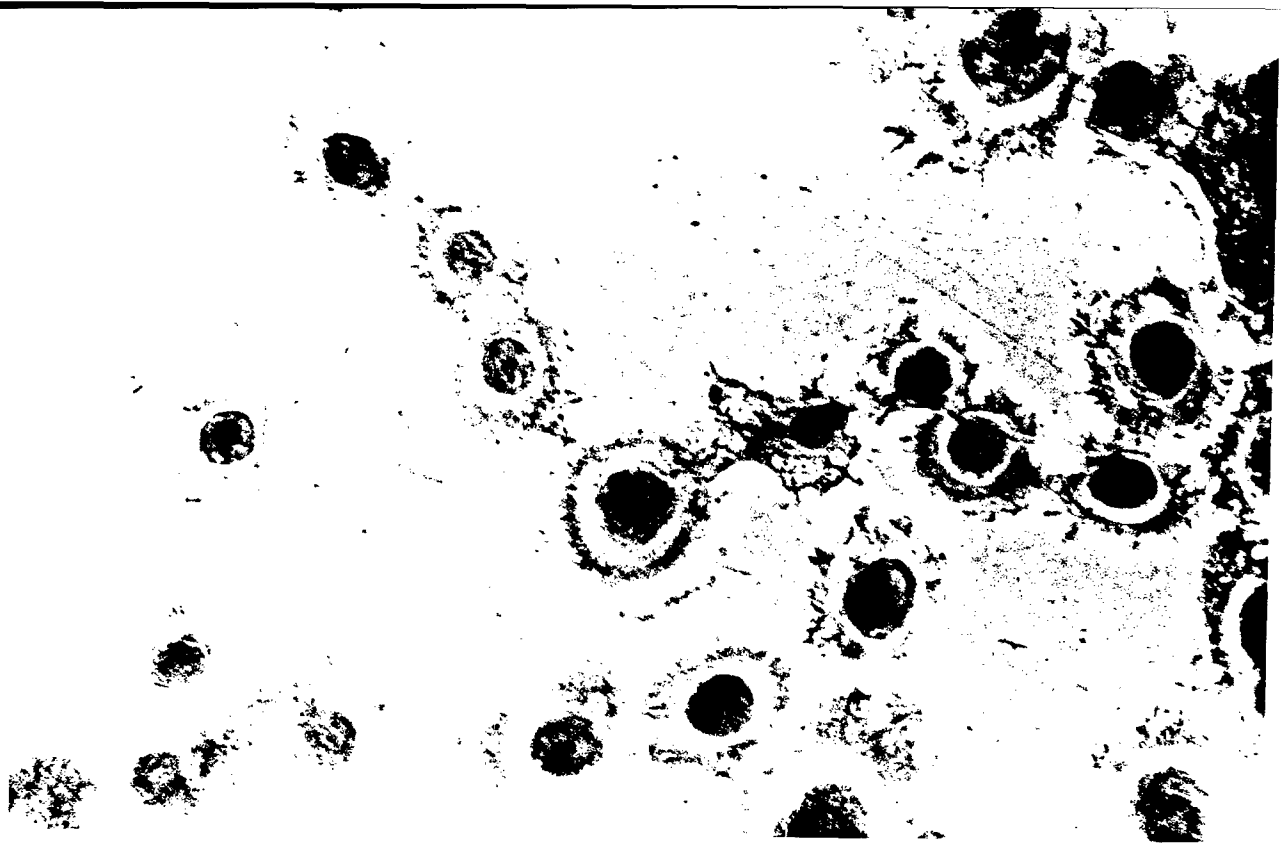
Keratinocytes obtained from excess human skin removed at the time of reduction mammoplasty were exposed to a range of concentrations of SM (0 - 1000 μM) over a 5 to 6 hr time course and observed for changes in morphology, cytoskeletal organization, and viability. In some experiments observations were extended to 24 hours to focus on effects which were induced by the lower concentrations of SM (≤ 250 μM). Keratinocytes under

control conditions tended to grow in clusters of cells which were in close association with each other. During the time course of SM injury, especially with higher concentrations of SM, this clustering of cells was largely lost (Figure 1).

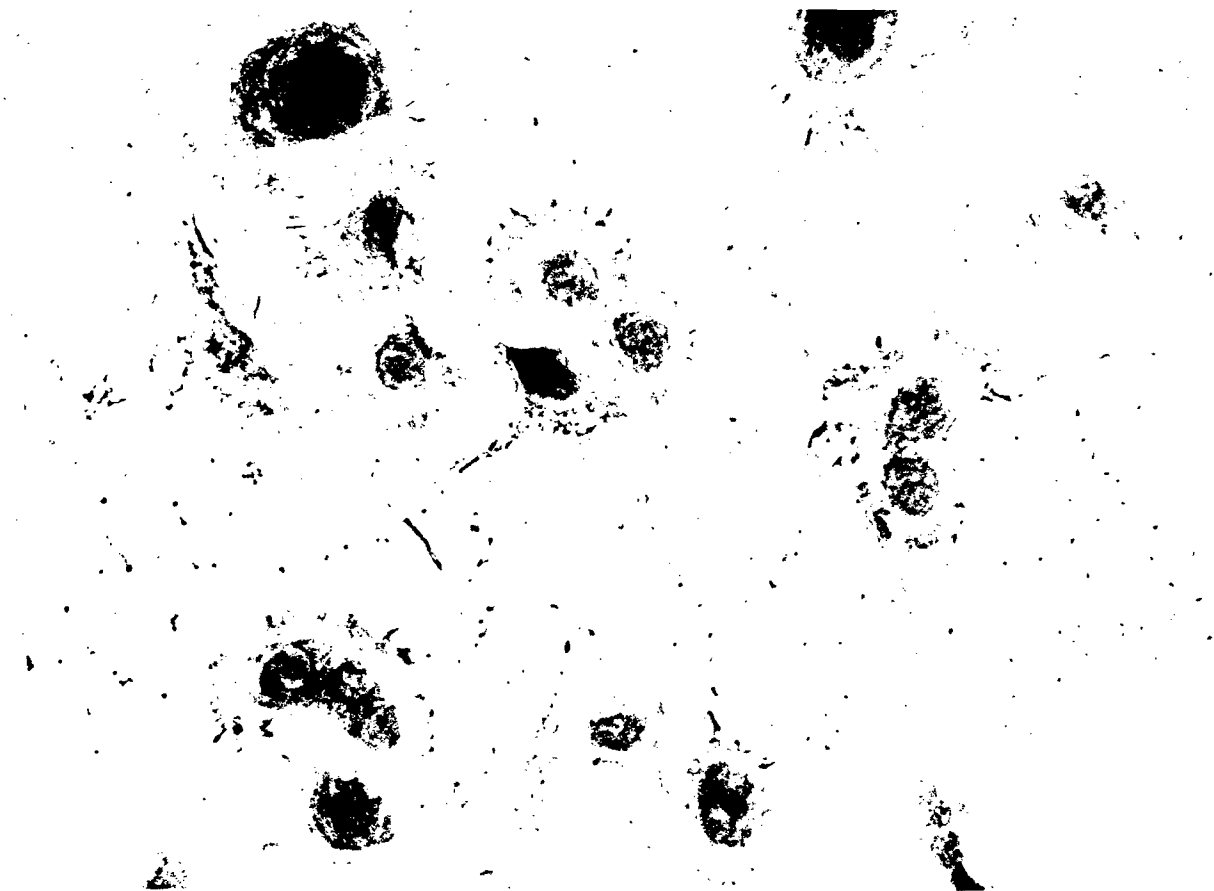
Initially, injured cells underwent swelling and rounding followed later by an apparent reduction in cell volume in nearly all cells injured with concentrations $\geq 250 \mu\text{M}$ SM by 2 to 3 hours after exposure to the agent. Similar morphologic changes occurred with lower concentrations of SM but developed more slowly and were only sporadic in their distribution (data not shown).



1 A



1B



1C

Figure 1. Micrographs of keratinocyte morphology after SM injury. The adherent cells were stained with Wright-Giemsa following exposure to SM. A) Control, uninjured cells at 3 hr. B) Cells 3 hr after exposure to 250 μ M SM. C) Cells 3 hr after exposure to 500 μ M SM. Note the altered morphology, i.e. apparent decrease in cytoplasmic density and loss of cell to cell contact after exposure to 250 μ M SM (B), a SM concentration associated with minimal loss of viability as compared to the control (A). Original magnification 400X.

When the SM-injured keratinocytes were evaluated with the acridine orange/ethidium bromide assay of viability and apoptotic nuclear features (17), significant loss of viability was only seen with SM concentrations $\geq 500 \mu\text{M}$ after 5 hours of injury (Figure 2). Viability 5 hours after SM exposure was $84.5 \pm 3.5\%$ ($p=0.02$, t test) for $500 \mu\text{M}$ SM and $67 \pm 6\%$ ($p=0.005$, t test) for $1,000 \mu\text{M}$ SM vs. $94 \pm 1.5\%$ for the uninjured control. None of the injured cells demonstrated apoptotic nuclear features, indeed all dead cells demonstrated nuclear and morphologic features consistent with a necrotic pattern of cell death in marked contrast to our earlier observations with endothelial cells which demonstrated both apoptosis and necrosis developing after exposure to SM concentrations $\geq 500 \mu\text{M}$ (15). Since in endothelial cells we had seen apoptosis as the dominant form of cell death at SM concentrations $\leq 250 \mu\text{M}$, we hypothesized that longer observations of the keratinocytes after exposure to lower concentrations of SM might demonstrate some evidence of apoptosis. We found minimal evidence at 24 hours of toxic keratinocyte death after exposure to concentrations of SM $\leq 250 \mu\text{M}$ (e.g. 16% of cells exposed to $250 \mu\text{M}$ SM were necrotic and only 2% apoptotic). The keratinocytes appeared to be remarkably resistant to induction of apoptosis. To further control for this we also exposed keratinocytes to ultraviolet (UV) irradiation as described in (13) and in our midterm report which induces nearly 100% of HL 60 cells to undergo highly synchronous apoptotic death over a 4 hour time course. Almost no effect on keratinocyte viability was induced by these conditions until the UV exposure time was doubled to 30 minutes. After 24 hours following this intense exposure to UV irradiation, ~ 25% of keratinocytes demonstrated the apoptotic nuclear features of chromatin compaction and clumping but also demonstrated loss of membrane integrity indicating that necrosis and apoptosis were occurring in the same cells. At later time points ≥ 48 hours, 40 - 50% of the cells were necrotic with 10 - 20% demonstrating the mixed pattern of apoptotic nuclear changes and loss of plasma membrane integrity. Thus, cultured human keratinocytes are remarkably resistant to induction of apoptosis by SM and UV. They exhibit an almost exclusively necrotic pattern

of death after SM exposure. The concentrations of SM which can induce necrosis and apoptosis in endothelial cells ($\geq 500 \mu\text{M}$) only induce necrosis in keratinocytes, whereas the concentrations of SM which induce apoptosis alone in endothelial cells ($\leq 250 \mu\text{M}$) (15) cause minimal loss of viability in keratinocytes and this is almost exclusively by necrosis.

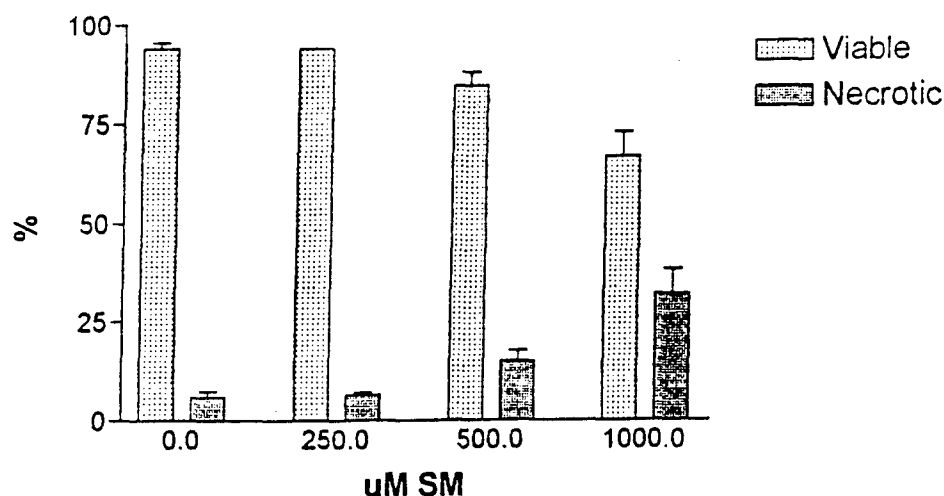
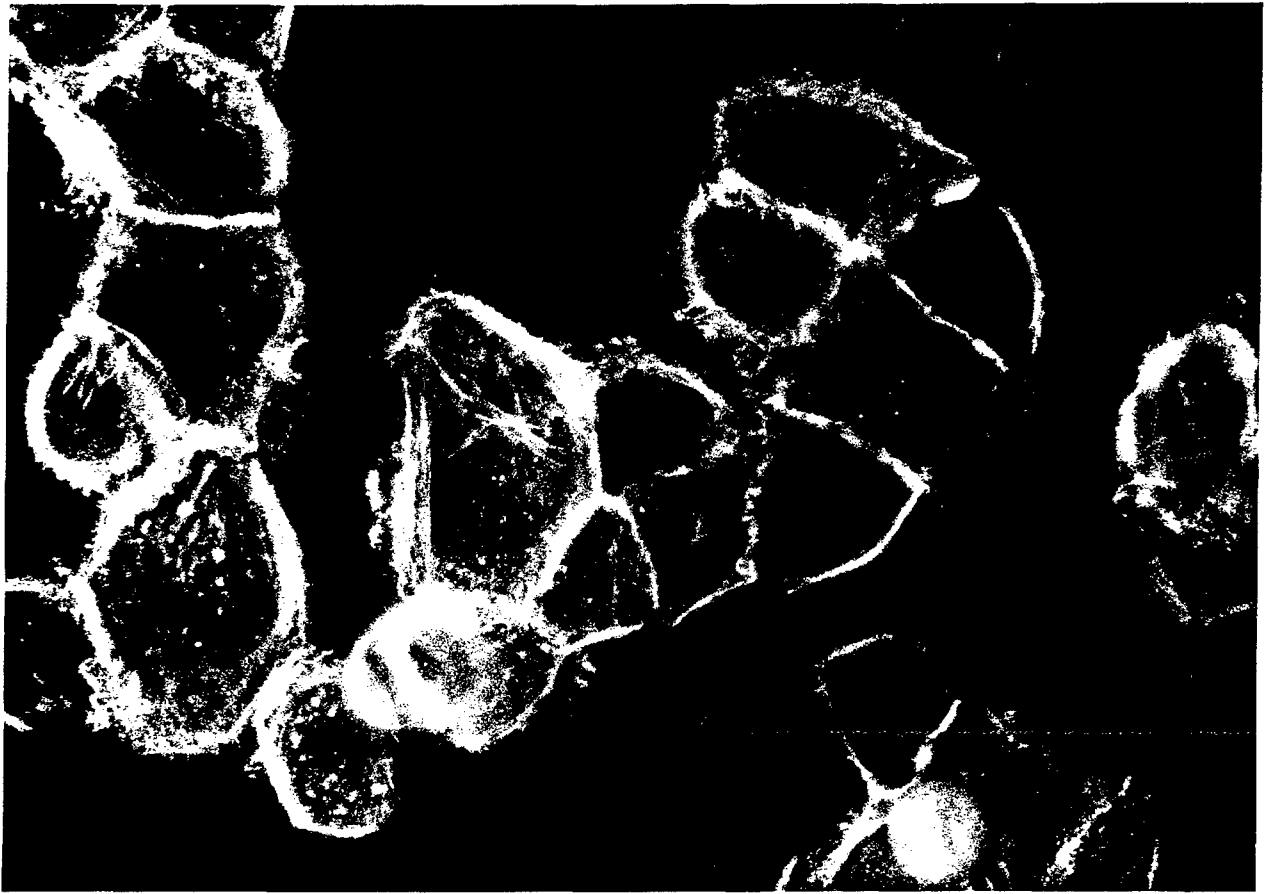
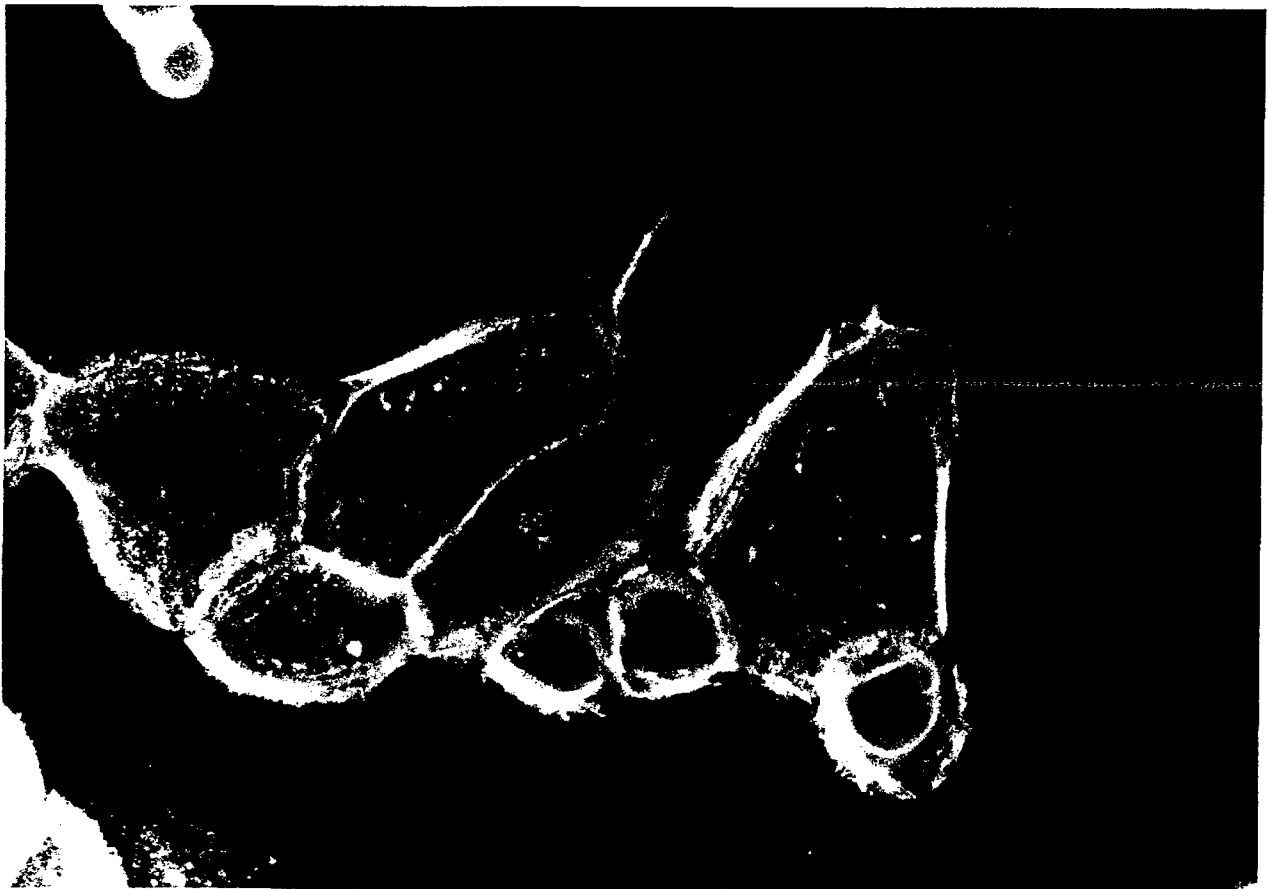


Fig. 2. Viability of keratinocytes 5 hrs after SM injury. Viability was assessed by the fluorescence microscopic assay of viability and apoptotic nuclear features (17). Each bar represents the mean of N = 3 separate determinations.

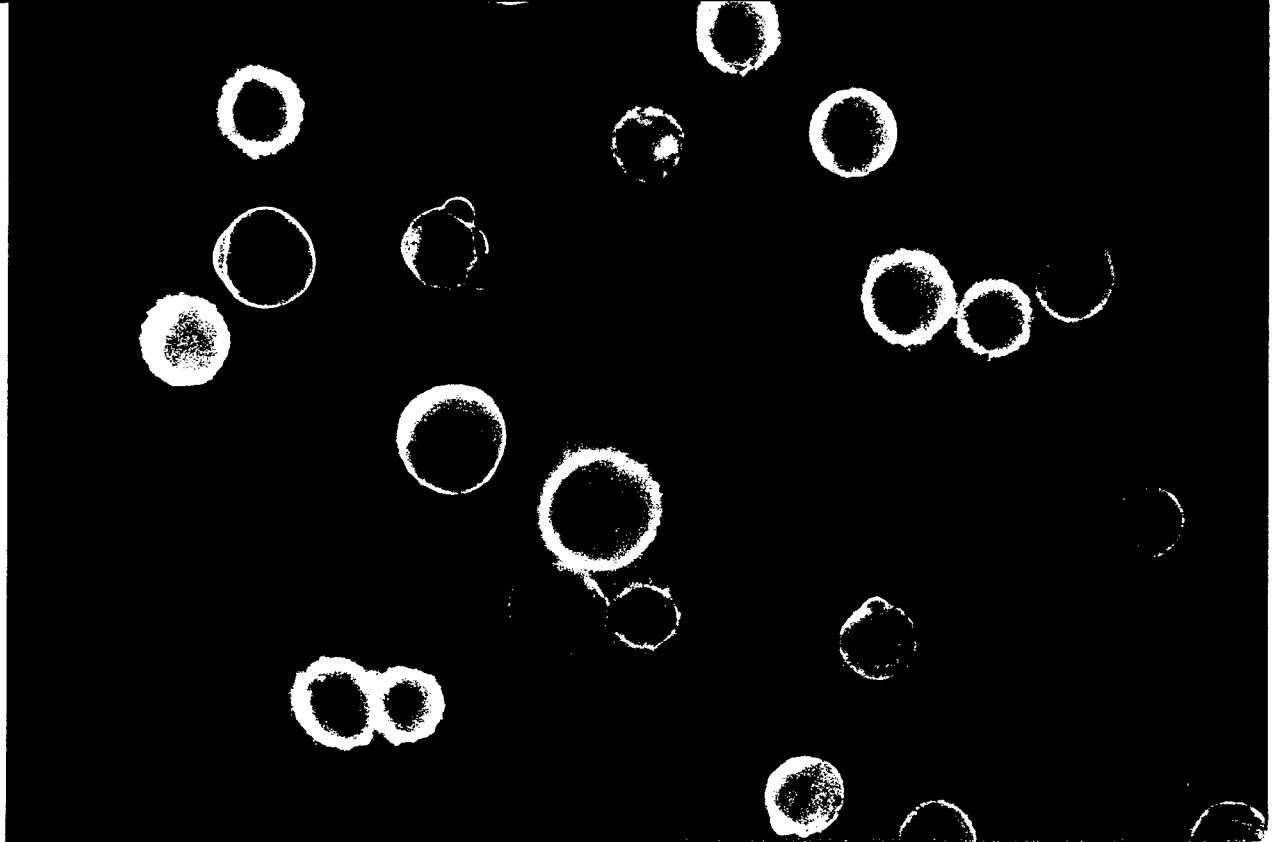
Keratinocytes fixed and stained with rhodamine phalloidin to visualize microfilaments (18) demonstrated a rich profusion of fine microfilaments particularly extending into cellular processes and at points of contact with other cells (Figure 3). By 2 - 2.5 hours after exposure to SM concentrations $\geq 250 \mu\text{M}$ surface blebbing, cell rounding, and loss of microfilament organization were common features of injured cells (Figure 3). Cell to cell contact was maintained fairly well at concentrations of SM ≤ 100



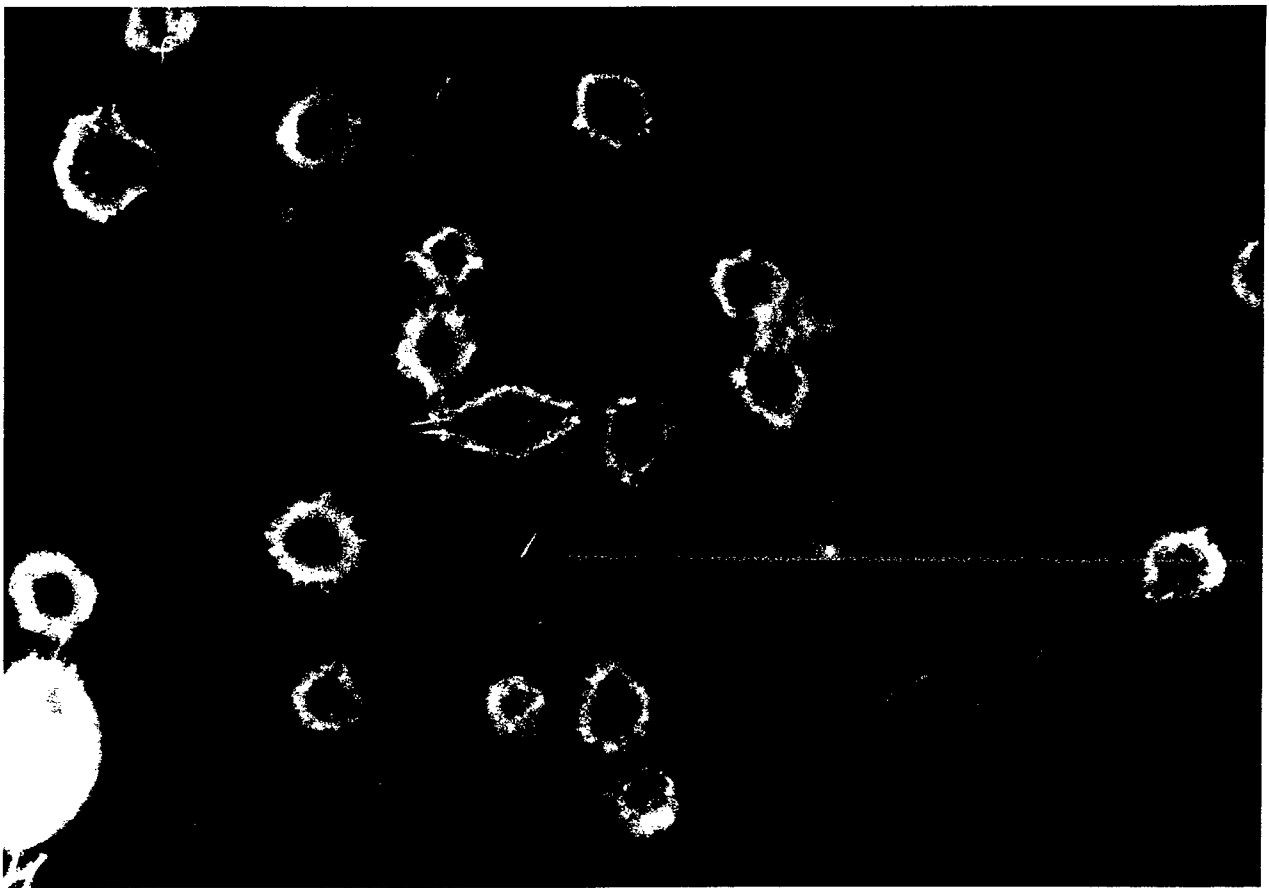
3A



3B



3C



3D

FIGURE 3. Fluorescence micrographs of keratinocytes stained with rhodamine phalloidin to visualize microfilaments. A) Control, uninjured cells at 2 hr; 400 X original magnification. B) Cells exposed to 100 μ M SM for 2.5 hr; 1000 X original magnification. C) Cells exposed to 250 μ M SM for 2.5 hr; 400 X original magnification. D) Cells exposed to 500 μ M SM for 2.5 hr; 400 X original magnification. Note the loss of fine microfilament architecture (especially at cellular junctions) at SM concentrations \geq 250 μ M and the absence of any perinuclear constricted bands of actin in the injured cells.

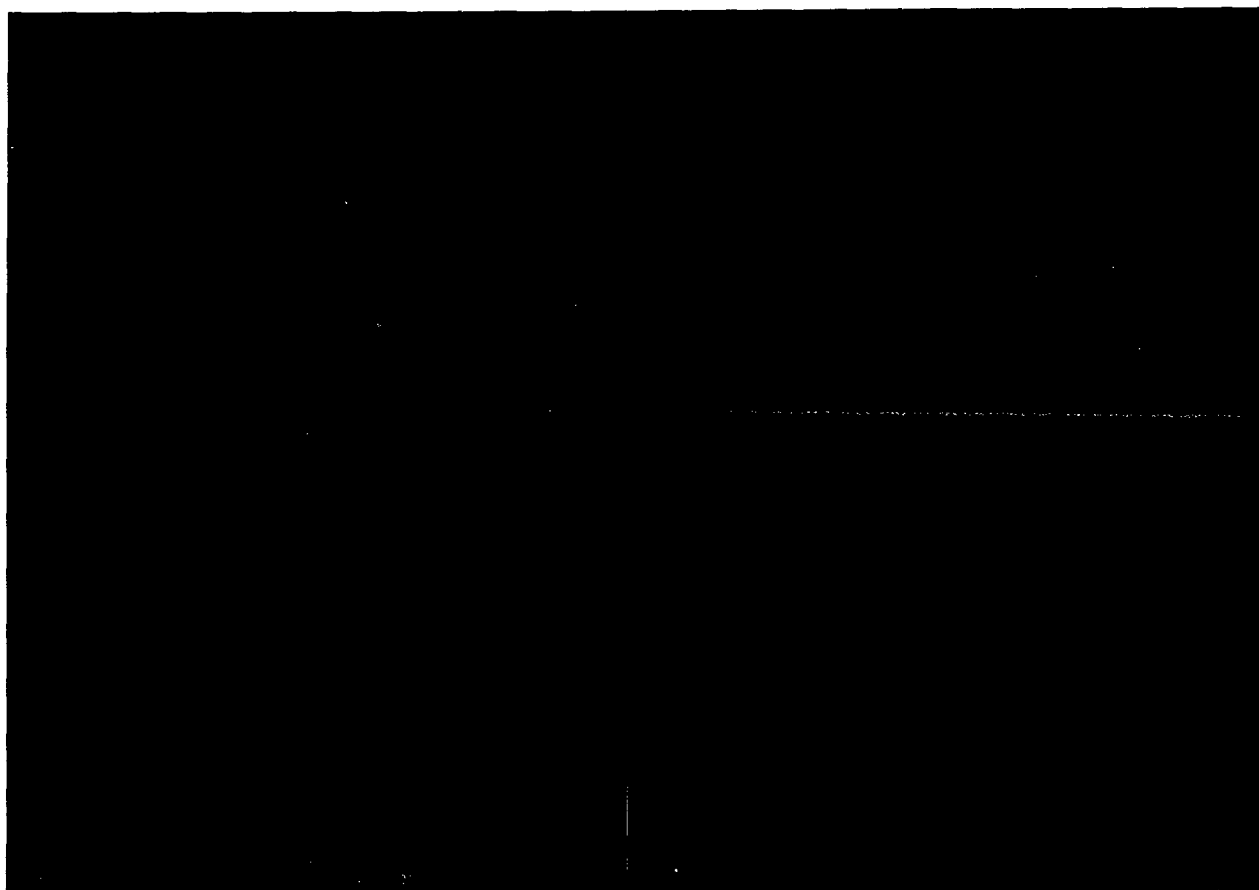
μM and correlated well with preservation of microfilament architecture, especially at cellular junctions (Figure 3). No constricted perinuclear bands of actin filaments could be identified in injured keratinocytes as had been seen in SM-injured endothelial cells (15). It is important to note that the morphologic and cytoskeletal (microfilament) changes induced by SM in keratinocytes occurred rapidly by 2 - 2.5 hours and with a concentration of SM (250 μM) not associated with loss of keratinocyte viability, suggesting that keratinocyte pathology associated with vesication may not depend upon cell death. Microtubules and intermediate filaments visualized by double antibody techniques, were altered by the higher concentrations of SM ($\geq 500 \mu\text{M}$) which were also associated with significant necrotic cell death. Microtubule depolymerization induced by $\geq 500 \mu\text{M}$ SM occurred at time points prior to onset of cell death and was accompanied by intermediate filament collapse around the nucleus (Figure 4). Thus, microfilaments appear to be the cytoskeletal structure in keratinocytes most sensitive to SM injury.



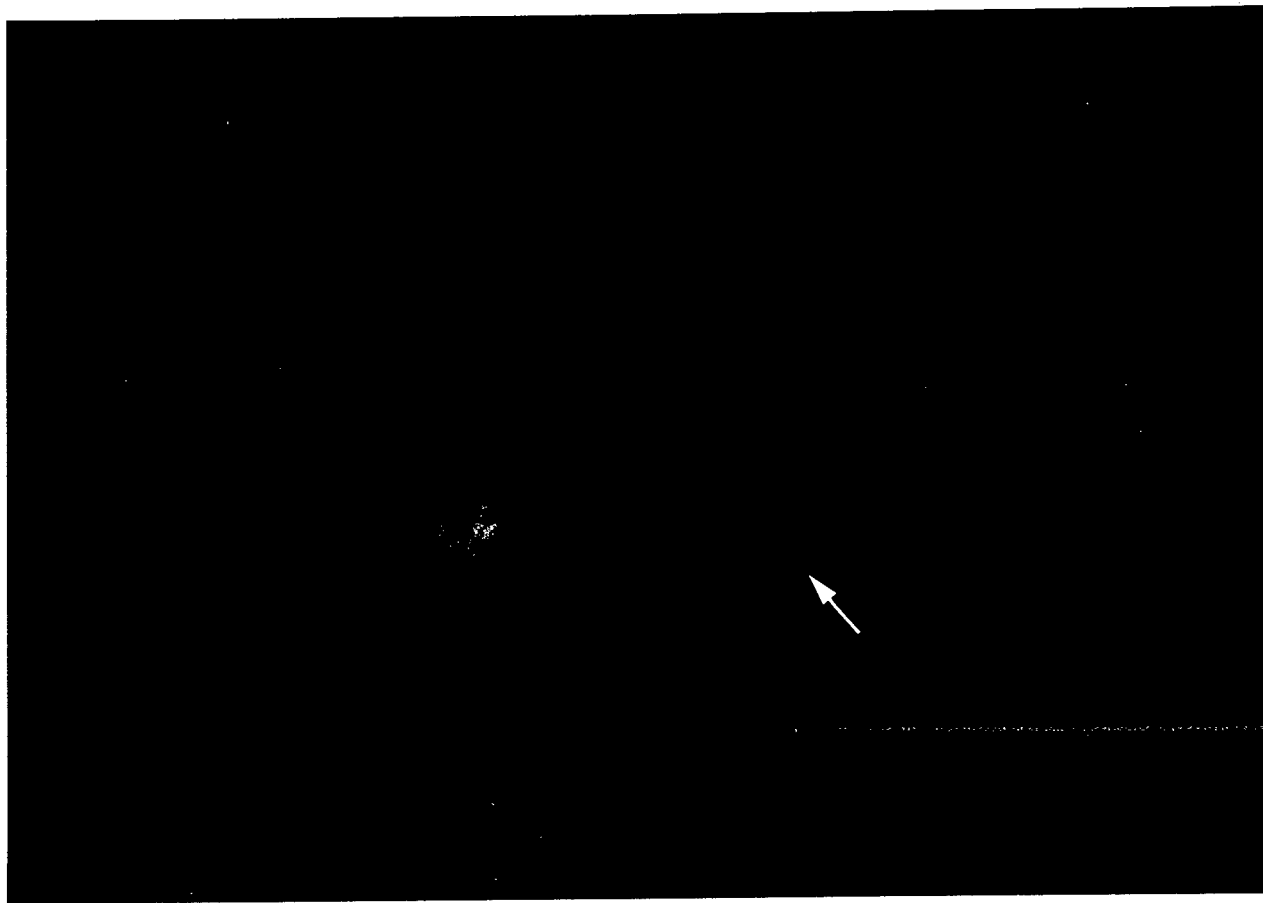
4A



4B



4C



4D

Figure 4. Fluorescence micrographs of keratinocytes stained using double antibody techniques for β tubulin in microtubules and cytokeratin in intermediate filaments. A) Control cells stained for microtubules. B) Cells exposed to 500 μ M SM for 2.5 hr stained for microtubules. C) Control cells stained for intermediate filaments. D) Cells exposed to 1000 μ M SM for 2.5 hr stained for intermediate filaments. Note depolymerization of microtubules and perinuclear collapse of intermediate filaments (arrow) after exposure to SM concentrations \geq 500 μ M; 400 X original magnification.

The effect of SM on keratinocyte ATP levels

In a pattern similar to the effect of SM on endothelial ATP levels (15), SM (\geq 500 μ M) reduced ATP levels (measured by the luciferin-luciferase assay) significantly by 5 hours in keratinocytes (Fig. 5). ATP levels in keratinocytes were reduced by \sim 50% or greater 5 hours after exposure to \geq 500 μ M SM ($p=0.0432$, ANOVA). The magnitude of the reduction in ATP was proportionately greater than can be explained purely on the basis of cell lysis alone (e.g. fig. 2 above). Consistent with the minimal toxicity seen at 5 hours with 250 μ M SM (e.g. fig. 2), ATP levels were largely unaffected by this concentration of SM (Fig. 5).

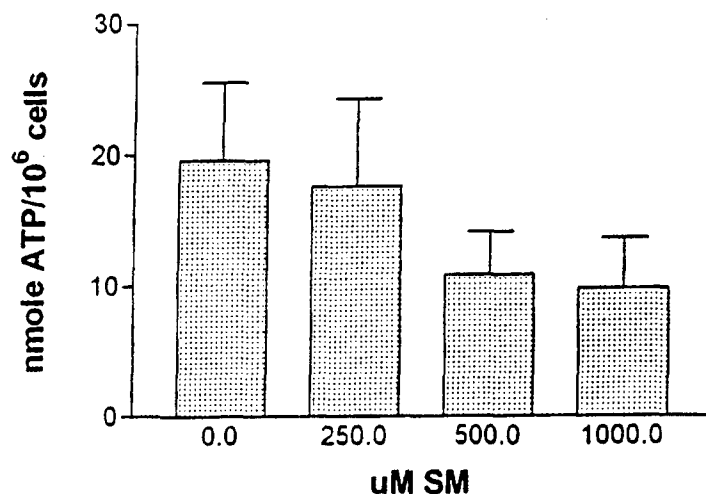


Fig.5. ATP levels (nmole/1x10⁶ cells) in keratinocytes 5 hrs after SM injury. ATP levels were measured using the luciferin-luciferase assay (15). Each bar represents the mean \pm S.D. of N = 4 separate determinations.

Glutamine supplementation and ATP levels in SM-

injured cells. To perform these experiments, the cells were incubated in medium to which final concentrations of 0, 2, and 4 mM glutamine were added 60 minutes before SM addition. ATP levels were then assayed 5 hr after SM injury using the luciferin-luciferase assay (15). The different concentrations of glutamine did not significantly alter control levels of ATP (fig. 6). The presence of glutamine did not prevent significant ($P=0.02$) reductions in endothelial ATP associated with SM concentrations ≥ 500 μ M (fig. 6). However, the presence of glutamine (2 mM was optimal) was essential for maintaining ATP levels in the control range in cells injured with 250 μ M SM (a concentration of SM associated with apoptosis only).

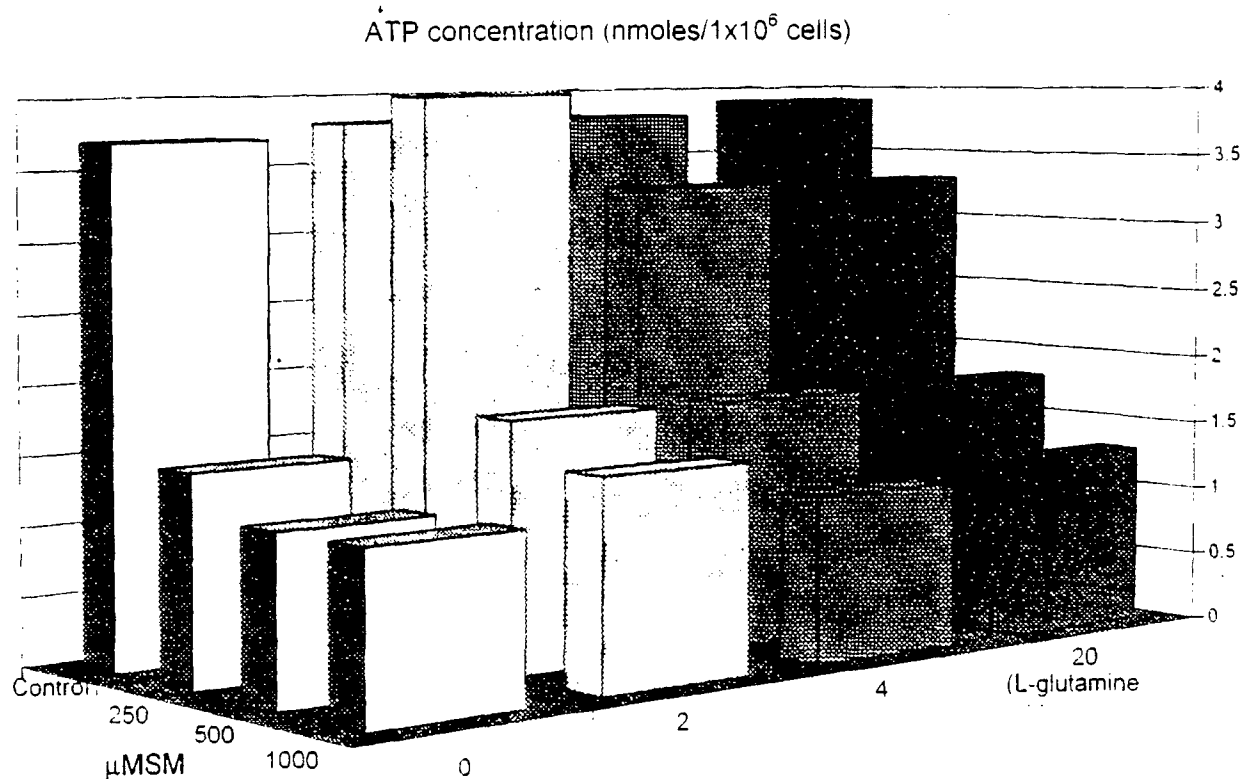


Fig. 6. The effect of glutamine supplementation on endothelial ATP levels during SM injury. The cells were treated as described in the text and ATP levels were assayed 5 hr after injury with 0-1000 μ M SM using the luciferin-luciferase assay (15). Each bar represents the mean of N = 3-5 separate determinations.

Keratinocyte ATP levels following SM injury were similarly unaffected by the presence or absence of glutamine (fig. 7). However, baseline (control) levels of ATP in keratinocytes were reduced by the experimental conditions of glutamine deprivation for 6 hr when compared to control ATP levels in Fig. 5 in which the controls did not experience any period of glutamine deprivation and had been grown continuously in 2 mM glutamine. Longer periods (18-24 hr) of glutamine deprivation resulted in keratinocyte death (data not shown).

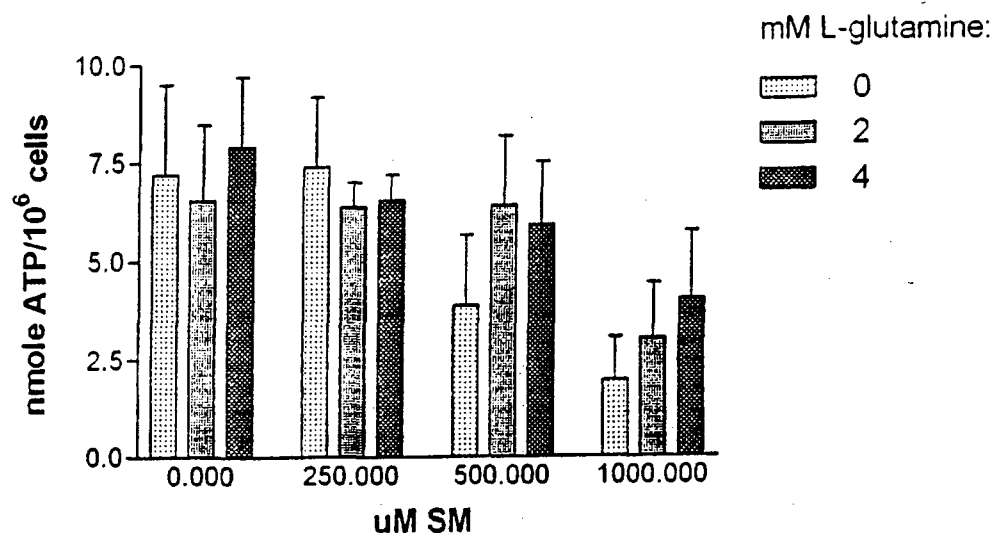


Fig. 7. The effect of glutamine supplementation on keratinocyte ATP levels during SM injury. The cells were treated as described in the methods and ATP levels were assayed 5 hr after injury with 0-1000 μ M SM using the luciferin-luciferase assay (15). Each bar represents the mean (\pm S.D.) of N = 3 separate determinations.

DNase I assay of filamentous (F)-actin in keratinocytes after SM injury

Previously we observed in the HL 60 cell line that the apoptotic form of cell death is characterized by a massive net depolymerization of F-actin as the cells shrink, undergo plasma membrane budding, and release apoptotic bodies (13). We also saw confirmation of this same pattern of actin depolymerization in SM-injured endothelial cells 6 hr after exposure to 1000 μ M SM, a concentration of the agent which produced rapid and synchronous development of apoptosis in the greatest number of cells thus making detection of this change possible with the relatively insensitive DNase I assay (15). We attempted to perform these same measurements with the DNase I assay in keratinocytes. Previous experience with epithelial-type cells (25) indicated that we should see a relatively large proportion of total actin as F-actin (i.e. G-actin as a percentage of total actin <50%).

We were unable for unclear reasons to effectively depolymerize F-actin in the keratinocyte samples with exposure to guanidine, which normally will completely depolymerize F-actin thus allowing measurement of total actin in this assay which depends on the ability of G-actin to inhibit DNase I (26). Under the standard assay conditions we were unable to measure total actin levels on multiple attempts that were much different from G-actin levels (only ~ 10% more) which if correct would indicate that the cells have a very small proportion of their actin as F-actin which is not consistent with the visible presence of many actin filaments in figure 3. Thus, further use of the DNase I assay in keratinocytes will require more work to determine why guanidine is relatively ineffective as an inducer of actin depolymerization in these cells. Fortunately, changes in F-actin can also be measured by SDS-PAGE of the detergent extract of cells. Using this methodology, we have been able to perform these measurements and also gain other information that the DNase I assay would not be able to provide (please see SDS-PAGE data below).

The effect of SM injury on NAD⁺ levels and the activity of poly-[ADP-ribose] polymerase (PARP) in endothelial cells and keratinocytes

The hypothesis that DNA alkylation by SM could activate PARP and thus consume NAD⁺ and help account for ATP loss after SM injury was tested in endothelial cells and keratinocytes. ADP-ribosylation of cellular protein was measured using ³H-NAD⁺ in digitonin-permeabilized cells as described in (20). At different time points after SM injury (2,3, & 5 hr), cells were washed and exposed to the radiolabelled substrate (³H-NAD⁺) for PARP under mild permeabilizing conditions (0.01% digitonin) to allow entry of ³H-NAD⁺ into the cells without causing cell lysis for a brief (5 min) incubation. The incubation was stopped with acid (trichloroacetic acid; TCA) precipitation and ADP-ribosylation was measured with a β counter as counts per minute (CPM) of radiolabel present in the acid precipitable material (protein) of the cells normalized to protein content. NAD⁺ levels over the same time course were measured using a spectrophotometric assay

(19) and also normalized to protein content and expressed as picomole NAD^+ /mg protein. The concentrations of 250 μM and 500 μM SM were chosen for these studies since the biologic effects in both keratinocytes and endothelial cells are quite different at these concentrations. In keratinocytes (e.g. fig. 2 & 5) little effect on viability or ATP is seen with 250 μM SM whereas 500 μM SM does exert significant effects on ATP and viability. In endothelial cells, the lower concentration of SM only causes apoptosis, whereas the higher concentration causes a mixture of apoptosis and necrosis and also significantly reduces ATP levels. Early in the time course (2 hr) there was a significant ($P=0.0185$, ANOVA) dose-dependent increase in PARP activity in endothelial cells after SM injury (fig.8). The activity of PARP remained elevated $\sim 4 \times$ over control throughout the time course in cells injured with 500 μM SM and was variably elevated after exposure to 250 μM SM (fig. 8). NAD^+ levels decreased in proportion to the increases in PARP activity in SM-injured endothelial cells (fig. 9), and there was a significant dose-related reduction in NAD^+ which occurred at 2 and 3 hours after SM exposure. Thus, there appeared to be a reciprocal relationship between PARP activity and NAD^+ levels in endothelial cells following SM injury and this was consistent with the hypothesis that SM-mediated DNA damage induces activation of PARP and subsequent consumption of NAD^+ .

When PARP activity was measured in keratinocytes after SM injury there was no significant injury-related increase in PARP activity seen (fig. 10). The baseline control level activity of PARP (normalized to protein content) was similar in keratinocytes to that observed in endothelial cells (fig. 10 compared with fig. 8). Although PARP activity did not change significantly, NAD^+ levels in keratinocytes fell significantly in a dose-dependent manner over the 5 hour time course of SM injury (fig. 11). It's not clear what process may account for the fall in NAD^+ levels in SM-injured keratinocytes in these experiments. It is conceivable that a transient, early increase in PARP activity prior to two

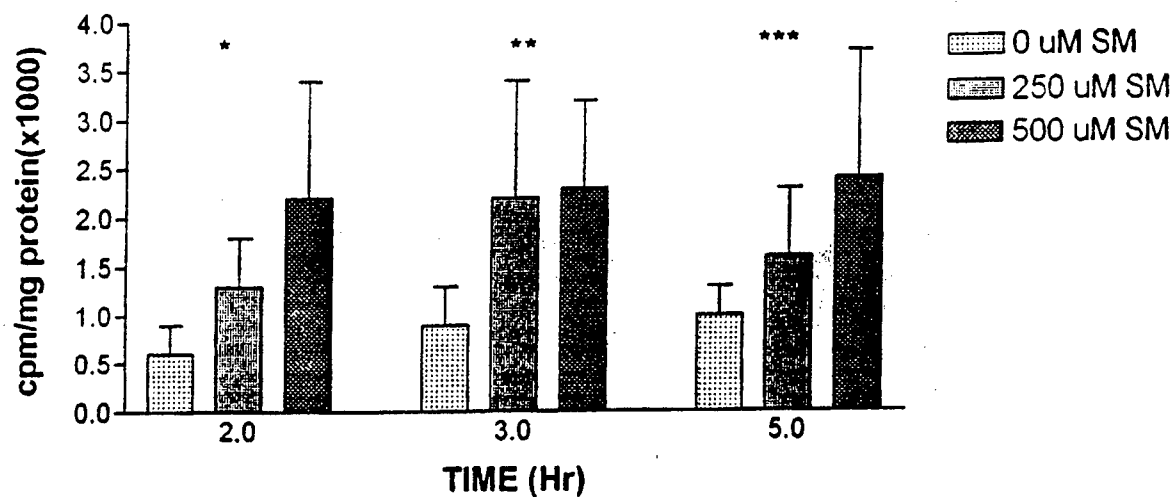


Fig. 8. Activity of poly-[ADP-ribose] polymerase (PARP) in endothelial cells after SM injury. PARP activity was measured by a brief (5 min) incubation of digitonin-permeabilized cells with ^3H -NAD at the time points indicated and the acid precipitable (protein) material counted in a β counter to determine incorporation of the radiolabel (20). Each bar represents the mean \pm S.D. of N = 4-5 separate determinations. The data are expressed as cpm/mg protein (x 1000). *, $P=0.0185$; **, $P=0.0574$; ***, $P=0.0824$; ANOVA.

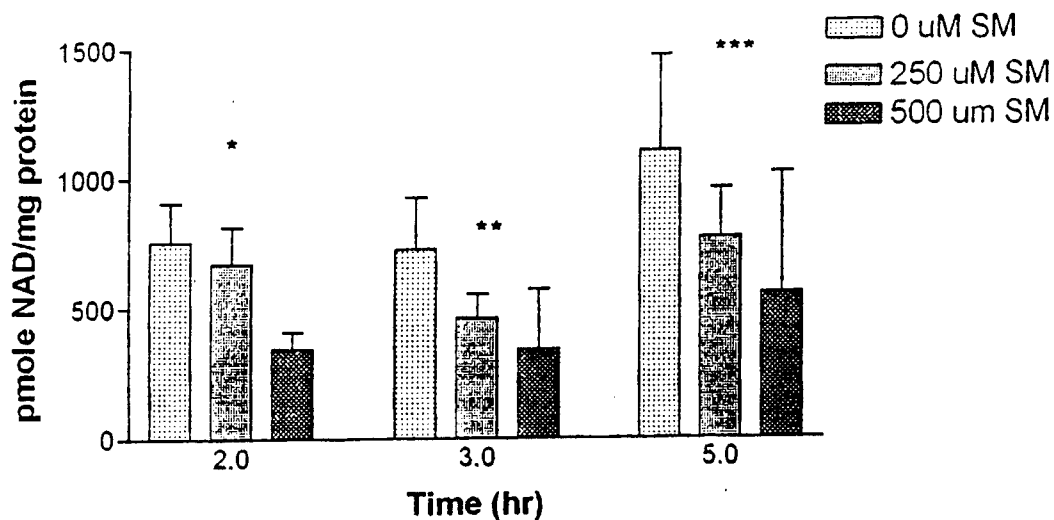


Fig. 9. NAD^+ levels in endothelial cells after SM injury. Cellular NAD^+ levels were measured spectrophotometrically (19). Each bar represents the mean \pm S.D. of N = 4-5 separate determinations. Data are expressed as pmole NAD^+ /mg protein. *, $P=0.0006$; **, $P=0.0235$; ***, $P=0.0889$; ANOVA.

hours might account for the fall in NAD levels in SM-injured keratinocytes. Others have seen a fall in NAD levels in cells after toxic injury independent of PARP activity and have postulated other mechanisms for the loss of NAD (such as activation of NAD kinase with subsequent interconversion of the pyridine nucleotide pool) (27). Also, NAD may be cleaved by NAD glycohydrolases as well as by PARP (28,29). Thus, one need not assume that NAD loss following toxic cellular injury is always a result of PARP activation.

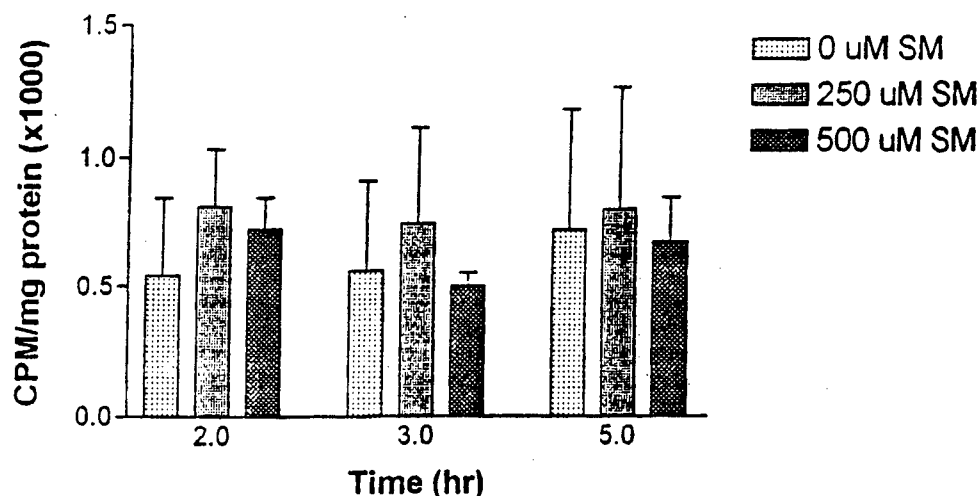


Fig. 10. Activity of poly-[ADP-ribose]-polymerase (PARP) in keratinocytes after SM injury. PARP activity was measured by a brief (5 min) incubation of digitonin-permeabilized cells with ^3H -NAD at the time points indicated and the acid precipitable (protein) material counted in a β counter to determine incorporation of the radiolabel (20). Each bar represents the mean \pm S.D. of N = 4-5 separate determinations. The data are expressed as cpm/mg protein (x 1000).

Changes in total glutathione (GSH) and oxidized GSH (GSSG) following SM injury in endothelial cells and keratinocytes

GSH and GSSG levels were measured enzymatically (22,23) in endothelial cells and keratinocytes after SM injury to examine the hypothesis that oxidant stress may be a part of the pathogenesis of SM-mediated cytotoxicity. Endothelial total GSH levels were minimally affected by SM injury (fig. 12A). SM also did not induce appreciable oxidation of GSH to GSSG in endothelial cells over control levels (fig. 12B). In contrast, SM injury reduced total GSH levels by ~ 30% in keratinocytes by 5 hr ($P=0.004$) without producing

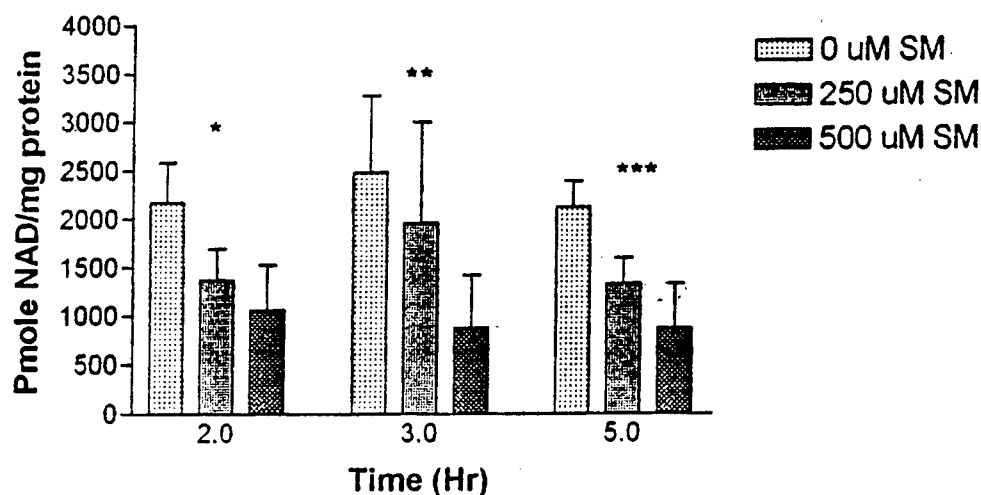


Fig. 11. NAD^+ levels in keratinocytes after SM injury. Cellular NAD^+ levels were measured spectrophotometrically (19). Each bar represents the mean \pm S.D. of N = 6-7 separate determinations. Data are expressed as pmoles NAD^+ /mg protein. *, $P=0.0041$; **, $P=0.044$; ***, $P=0.0001$; ANOVA.

any significant effect on levels of GSSG (fig. 13). These data suggest that metabolism of SM may differ between endothelial cells and keratinocytes and that intracellular oxidant generation and/or sulfhydryl (SH) oxidation might be induced in keratinocytes but not in endothelial cells by SM exposure. Other more direct means of detecting intracellular oxidant generation in SM-injured keratinocytes will be needed for future studies since reduction of total GSH levels alone is at best an indirect measure of intracellular oxidant generation.

Sodium dodecyl sulfate - polyacrylamide gel electrophoretic (SDS-PAGE) analysis of the endothelial and keratinocyte cytoskeleton after SM injury

We have previously shown that although a large portion of the cell cytoskeleton is contained in the detergent (triton x-100)-insoluble cellular extract, a significant portion remains soluble in triton x-100 (7). We have also shown that when the detergent extract of

the cytoskeleton is separated by SDS-PAGE under non-reducing conditions [without β mercaptoethanol (β ME) present] S-S cross linking induced by SH oxidation of cytoskeletal

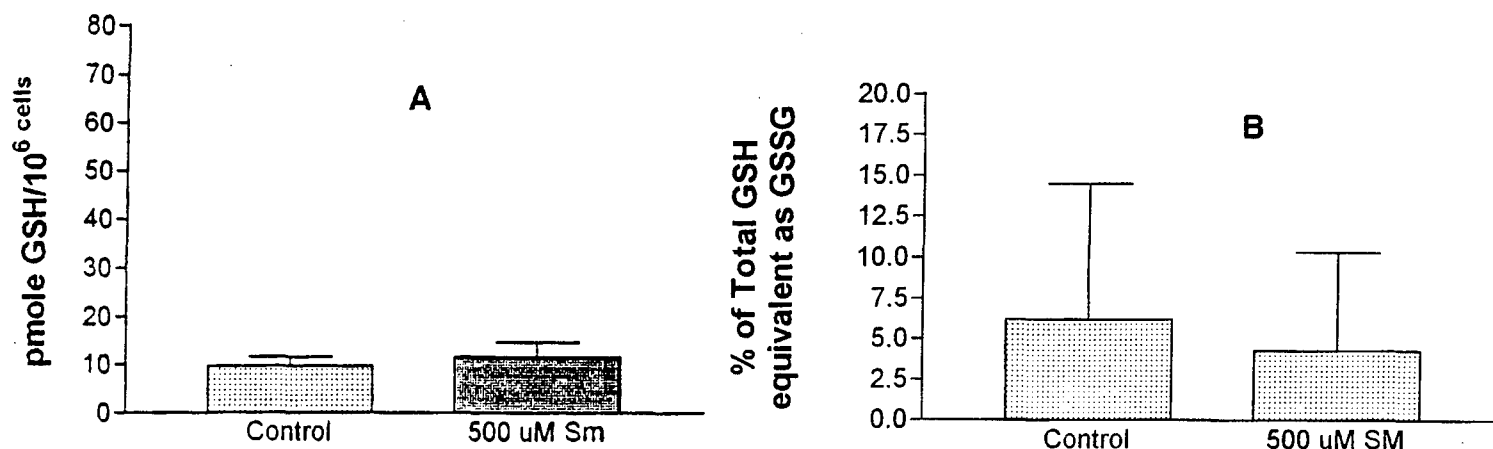


Fig. 12. Total GSH (A) and GSSG levels (B) in endothelial cells 5 hr after SM injury. Total GSH and GSSG were measured enzymatically (22,23) and expressed as pmole GSH/ 1×10^6 cells or for GSSG, the percentage of total GSH equivalents as GSSG. Each bar represents the mean \pm S.D. of N = 5 separate determinations.

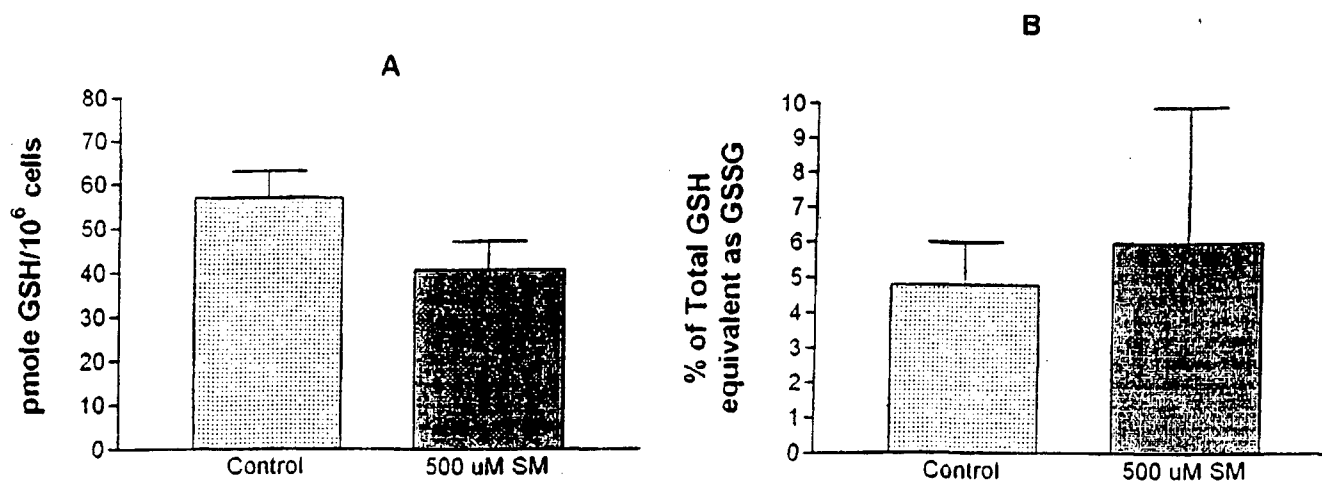
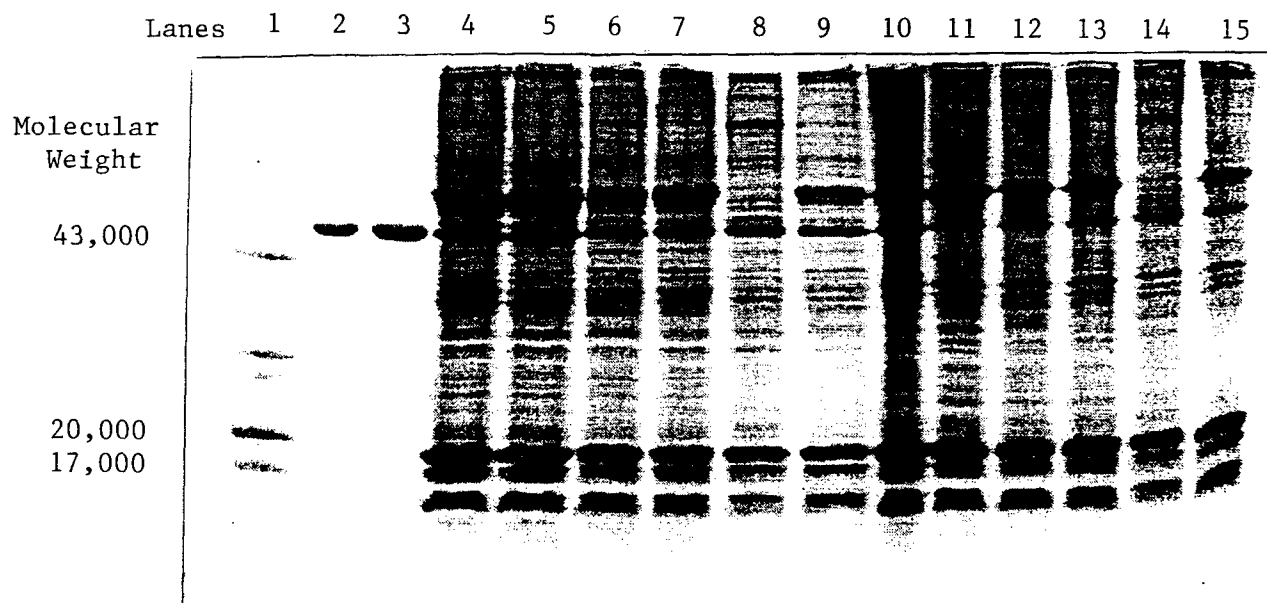
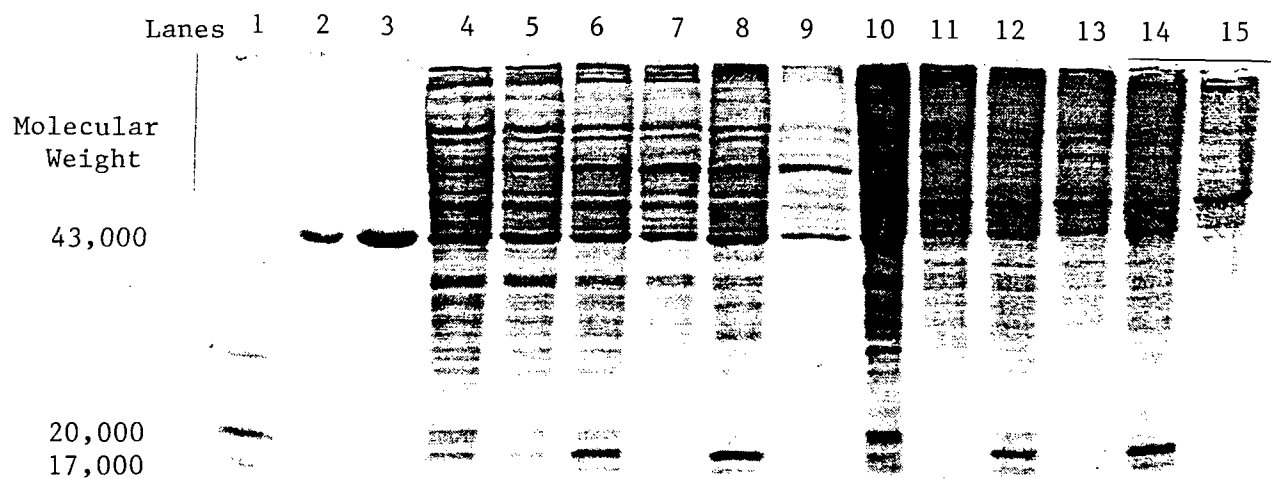


Fig. 13. Total GSH (A) and GSSG levels (B) in keratinocytes 5 hr after SM injury. Total GSH and GSSG were measured enzymatically (22,23) and expressed as pmole GSH/ 1×10^6 cells or for GSSG, the percentage of total GSH equivalents as GSSG. Each bar represents the mean \pm S.D. of N = 5 separate determinations.



14A



14B

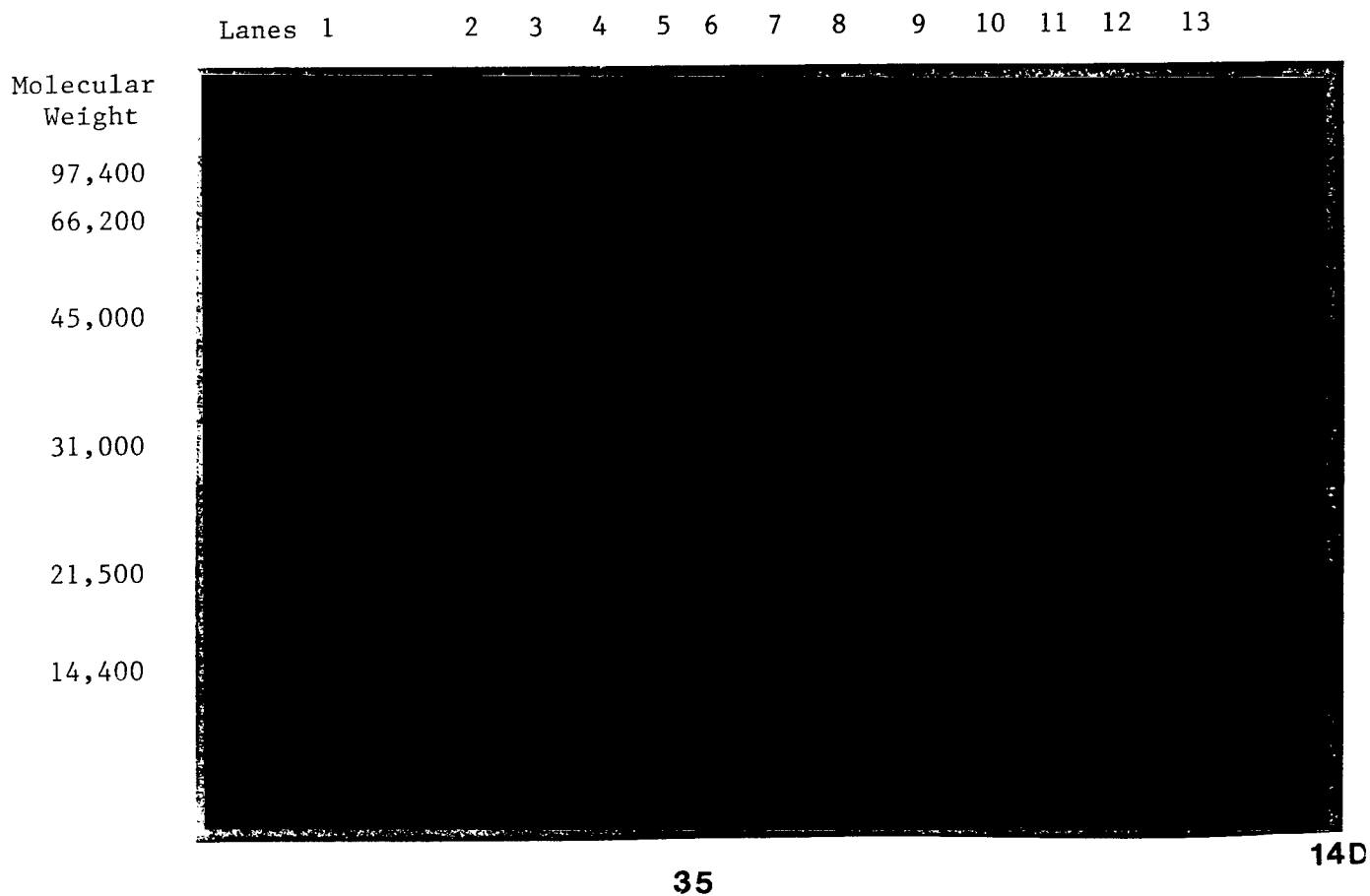
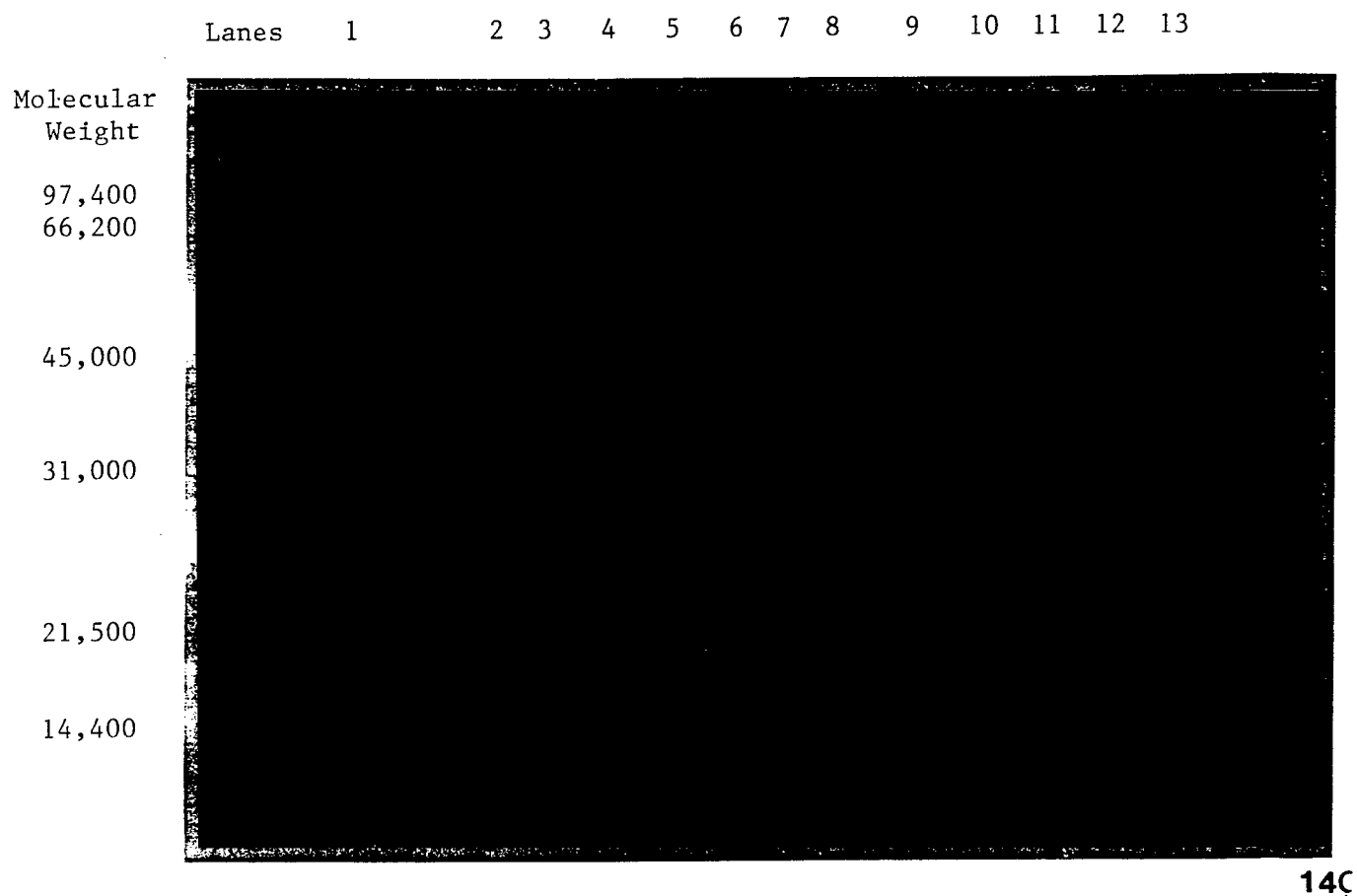


Figure 14. 12% SDS-PAGE of Tx-100-insoluble and -soluble cytoskeletal extracts of endothelial cells and keratinocytes. After 5 hr of injury, adherent cells which were or were not pretreated with 50 mM NAC were extracted with 1% Tx-100 and the detergent-insoluble and -soluble cytoskeletal extracts were separated on 12% SDS-PAGE +/- β ME. A) 12% SDS-PAGE of the triton-x-100-insoluble extract from endothelial cells 5 hr after SM injury. Lanes: 1 = myosin light chain — 17-20 kD bands (and contaminating larger proteins from chicken muscle; Sigma); 2 & 3 = actin standards (5 & 10 μ g respectively); 4,6,8 = control, 250 and 1000 μ M SM samples respectively, run under reducing conditions (+ β ME); 5,7,9 = control, 250, and 1000 μ M SM samples respectively, with 50 mM NAC pretreatment also run under reducing conditions (+ β ME); 10,12,14 = control, 250, and 1000 μ M SM samples respectively, run under non-reducing conditions (--- β ME); 11,13,15 = control, 250, and 1000 μ M SM samples respectively, pretreated with 50 mM NAC and run under non-reducing conditions (--- β ME). B) 12% SDS-PAGE of the triton-x-100-soluble extract from endothelial cells 5 hr after SM injury (from the same representative experiment as in A). Lanes: 1 = myosin light chain ~ 17-20 kD bands (and contaminating larger proteins from chicken muscle; Sigma); 2 & 3 = actin standards ~ 43kD (5 & 10 μ g respectively); 4,6,8 = control, 250 and 1000 μ M SM samples respectively, run under reducing conditions (+ β ME); 5,7,9 = control, 250, and 1000 μ M SM samples respectively, with 50 mM NAC pretreatment also run under reducing conditions (+ β ME); 10,12,14 = control, 250, and 1000 μ M SM samples respectively, run under non-reducing conditions (— β ME); 11,13,15 = control, 250, and 1000 μ M SM samples respectively, pretreated with 50 mM NAC and run under non-reducing conditions (---- β ME). C) 12% SDS-PAGE of the triton x-100-insoluble extract from keratinocytes 5 hr after SM injury. Lanes: 1 = molecular weight markers in descending order: 97.4 kD, 66.2 kD, 45 kD, 31 kD, 21.5 kD, and 14.4 kD; 2,4,6 = control, 250, and 1000 μ M SM samples respectively, run under non-reducing conditions (- β ME); 3, 5,7 = control, 250, and 1000 μ M SM samples respectively, pretreated with 50 mM NAC and run under non-reducing conditions (- β ME); 8,10,11 = control, 250, and 1000 μ M SM samples respectively, run under reducing conditions (+ β ME); 9,13,12 = control, 250, and 1000 μ M SM samples respectively, pretreated with 50 mM NAC and run under reducing conditions (+ β ME). D) 12% SDS-PAGE of the triton x-100-soluble extract from keratinocytes 5 hr after SM injury (from the same representative experiment as in C). Lanes: 1 = molecular weight markers in descending order: 97.4 kD, 66.2 kD, 45 kD, 31 kD, 21.5 kD, and 14.4 kD; 2,4,6 = control, 250 & 1000 μ M SM samples respectively, run under non-reducing conditions (- β ME); 3,5,7 = control, 250 & 1000 μ M SM samples respectively, pretreated with 50 mM NAC and run under non-reducing conditions (- β ME); 8,10,12 = control, 250 & 1000 μ M SM samples respectively, run under reducing conditions (+ β ME); 9,11,13 - control, 250 & 1000 μ M SM samples respectively, pretreated with 50 mM NAC and run under reducing conditions.

proteins can prevent large aggregates of the oxidized cytoskeletal proteins from entering the gel (30). Using these methods, we examined the Tx-100-insoluble and -soluble extracts of endothelial cells and keratinocytes 5 hours after SM injury. Parallel experimental samples were analyzed from cells pretreated with 50 mM NAC, since this agent can prevent apoptotic death in endothelial cells exposed to SM (16) and also serve as a potential SH donor during oxidative stress. Figure 14A depicts a representative SDS-PAGE of the triton x-100-insoluble material from endothelial cells 5 hours after exposure to 0, 250, & 1000 μ M SM with and without pretreatment with 50 mM NAC and run under reducing and non-reducing conditions (+/- β ME). There was a dose-related loss of actin (~ 20% for 250 μ M SM and ~ 40% for 1000 μ M SM vs. the control) which was not altered by pretreatment with NAC as determined by scanning densitometry of the respective actin

bands. These observations are consistent with the actin depolymerization previously reported for apoptotic cell death (13). Of particular interest is that NAC pretreatment which prevents the nuclear changes of apoptosis and the constriction of the peripheral cortical band of actin in SM-injured endothelial cells did not prevent the actin depolymerization. This suggests that NAC pretreatment may not be blocking all aspects of the cytopathologic changes which occur during apoptosis. NAC pretreatment dramatically inhibited loss of a ~ 55-60,000 m.w. band induced by 1000 μ M SM. Minimal if any evidence for large S-S cross linked protein aggregates could be found in the non-reduced samples.

Figure 14B depicts the SDS-PAGE of the triton x-100-soluble material from endothelial cells in the same representative experiment depicted in figure 14A. Similar results with respect to levels of actin in the detergent-soluble pool of actin were found as those seen in the detergent-insoluble pool of actin following SM injury described above. Again, NAC pretreatment did not prevent the SM-induced changes in actin in this pool of actin. Of particular interest, an ~ 20,000 m.w. band (which may correspond to the myosin light chain) became enriched following injury with either 250 or 1000 μ M SM. NAC pretreatment prevented this phenomenon. Myosin light chain movement into the detergent-soluble cytoskeletal pool may be an important concomitant of the contraction process which may permit the perinuclear constriction of the cortical band of actin (15).

Figure 14C depicts the SDS-PAGE analysis of the triton x-100-insoluble material extracted from keratinocytes 5 hours after SM injury run under reducing and non-reducing conditions with and without NAC pretreatment. Both concentrations of SM (250 & 1000 μ M) were associated with a small loss of actin (9.4 and 12.6% reductions, respectively) from the detergent-insoluble cytoskeletal extract of the keratinocytes run under reducing conditions. Similar reductions in other protein bands were also seen under these conditions. NAC pretreatment of the keratinocytes alone was associated with a 16% decrease in F-actin in the detergent-insoluble pool (estimated from scanning densitometry). This effect of NAC pretreatment was not seen with the endothelial cells. Of particular

interest was the presence of high molecular weight aggregates of protein at the top of the gel in lanes of injured samples run under non-reducing conditions which is strongly suggestive of S-S cross linking of cytoskeletal proteins (30) most likely secondary to oxidant stress (Table 1). NAC pretreatment did not prevent this phenomenon although it appears to have decreased its magnitude slightly (fig. 14C). SDS-PAGE analysis of the triton x-100-soluble cytoskeletal extract from keratinocytes after SM injury (fig. 14D) again revealed that NAC pretreatment alone also resulted in a decrease in protein content in this cytoskeletal pool of keratinocytes. It was particularly interesting to again see the large

TABLE 1

	<u>-βME</u>	<u>+βME</u>
250 μM SM	+32.5 %	+0.5 %
1,000 μM SM	+102.1 %	+23.7%

Table 1. Percentage increase of relative optical density (ROD) of Coomassie-stainable material from the TX-100-insoluble cellular extract not entering the polyacrylamide gel in Fig. 14C measured as described in the methods. The ROD was determined by scanning densitometry and the difference between the control and injured value was then expressed as a percentage (increase) of the control value. Note the much greater amount of material present under non-reducing (-βME) conditions.

molecular weight aggregates at the top of the gel in lanes of SM-injured samples run under non-reducing conditions (fig. 14D). Thus, measurable loss of total GSH and the presence of high molecular weight S-S cross linked aggregates demonstrable on SDS-PAGE analysis of cytoskeletal proteins run under non-reducing conditions in SM-injured keratinocytes are evidence suggestive that oxidant generation within the cells is a component of SM injury. Such evidence is lacking in endothelial cells following SM exposure and suggests that different cellular metabolic responses to the agent may govern this phenomenon.

Functional correlates of SM injury - adherence and endothelial permeability barrier function.

As was presented in the midterm report, endothelial cell adherence characteristics are altered substantially by SM concentrations $\geq 500 \mu\text{M}$ (15). Keratinocyte adherence is also markedly diminished by SM injury and decreases significantly in a dose-related manner even at concentrations of $250 \mu\text{M}$ SM which are not associated with significant loss of viability (fig. 15).

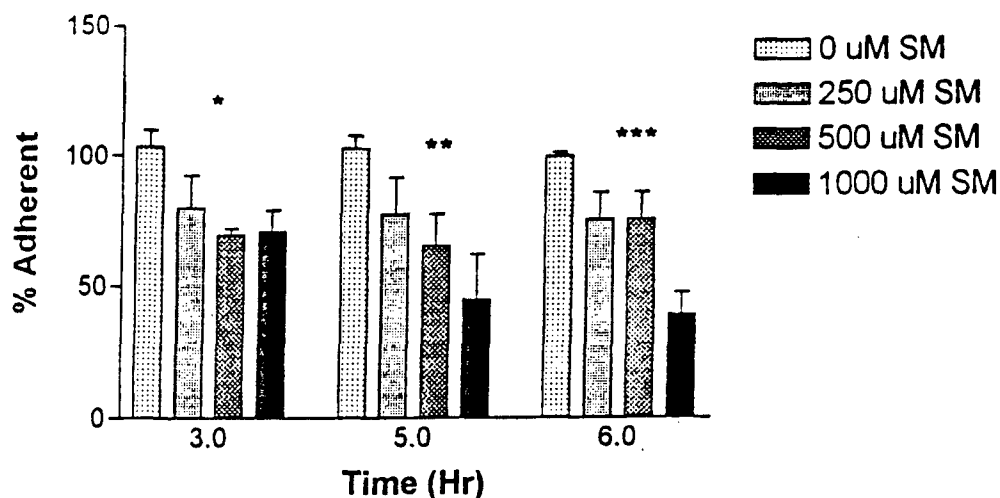


Fig. 15. Keratinocyte adherence during the time course of SM injury. At each time point the media was removed, the cells were harvested with 0.05% trypsin and 0.02% EDTA, and counted using an hemocytometer (15). The data are expressed as a percentage of cell number at time zero. Each bar represents the mean \pm S.D. of N = 3 separate determinations. *, $P=0.0203$; **, $P=0.0219$; ***, $P=0.0009$; ANOVA.

We also examined the ability of confluent endothelial monolayers grown on Transwell (Costar) plates to act as model permeability barriers after SM injury. Briefly, 3.5 hours after SM injury 1% albumin in RPMI media (to which no phenol red had been added) was added to the upper chamber of the well. The lower chamber only had RPMI (minus phenol red). At different time points 100 μl samples were taken from the lower chamber and added to 1 ml of a colorimetric albumin reagent (bromocresol green; Sigma) and the absorbance which was proportional to albumin content was read at 628 nm on a spectrophotometer. Data have been expressed as a percentage of the absorbance of 100 μl

of 1% albumin (i.e. conditions equal to the albumin concentration in the upper chamber at the beginning of the assay). Figure 16 demonstrates a significant dose-related increase in albumin flux after SM injury and that concentrations of SM associated with endothelial apoptosis alone (i.e. 250 μ M SM) are sufficient to produce significant disruption of barrier function. Thus, cell lysis is not necessary for the development of conditions which could support the capillary leak and fluid accumulation necessary for vesication to develop. Preliminary observations (data not shown) also suggest that NAC pretreatment in this model partially mitigates the effects of SM on barrier permeability, further supporting the concept that apoptosis (which is NAC-sensitive) may alone be sufficient to cause capillary leak after SM injury.

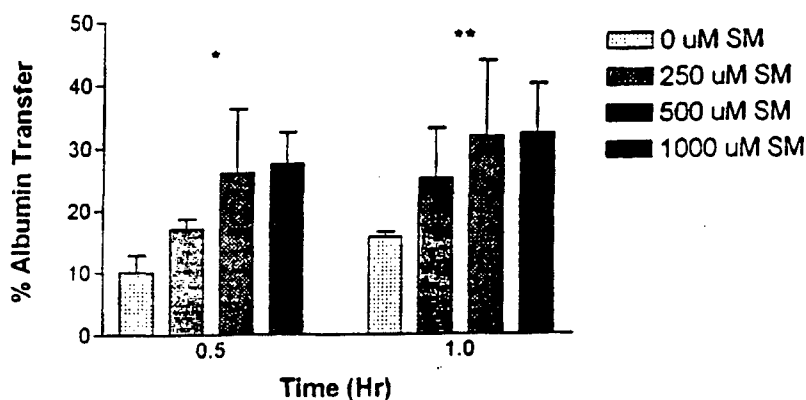


Fig. 16. Permeability barrier function of endothelial monolayers after SM injury. Albumin flux across endothelial monolayers after injury with 0-1000 μ M SM was measured as described in the text. Measurements started at 3.5 hr after SM injury were performed over a time course of 30 and 60 min. Data are expressed as a percentage of the maximal absorbance of the 1% albumin solution in the upper well at the beginning of the assay. Each bar represents the mean \pm S.D. of N = 4 separate determinations. *, $P=0.0072$; **, $P=0.0599$; ANOVA.

CONCLUSIONS.

The primary goal of this contract has been to characterize the nature of cell injury and death induced in endothelial cells and keratinocytes by SM to form a basis for understanding the pathogenic mechanisms responsible for SM-induced vesication. SM can induce two different forms of cell death in endothelial cells, apoptosis and necrosis (15).

The two patterns of endothelial cell death are characterized by profound changes in the endothelial cytoskeleton which are correlated with equally dramatic alterations of endothelial morphology and adherence characteristics. Metabolic effects on endothelial ATP and NAD⁺ were most pronounced at concentrations of SM (e.g. 500 μ M) associated with a mixed pattern of necrotic and apoptotic death. PARP activity in endothelial cells increased in response to SM injury in a dose-dependent fashion and may help to account for the NAD⁺ loss and indirect effects on ATP levels. Pretreatment overnight with 50 mM NAC allowed us to more precisely define those elements of SM injury in endothelial cells characteristic of apoptosis (especially the microfilament pathology) (15). Polyacrylamide gel electrophoretic analysis of the endothelial cell cytoskeleton confirmed DNase I measurements (15) showing a net (loss) depolymerization of actin filaments by 5-6 hr after SM injury in endothelial cells, a feature also seen in other models of apoptotic cell death (13). The changes in the 60 kD and 20 kD proteins induced by SM (Figures 14A & B) and prevented by pretreatment with NAC may be important clues to deciphering the series of biochemical events responsible for cytoskeletal contraction and its associated cellular shrinkage and rounding. Endothelial monolayers acting as model permeability barriers are sensitive to SM injury — the greatest leak occurring at concentrations producing the greatest (i.e. most rapid and synchronous) changes in endothelial morphology as well as loss of adherence (15). Concentrations of SM (e.g. 250 μ M) associated only with apoptosis are sufficient to significantly alter permeability barrier function.

Keratinocytes represent a marked contrast to endothelial cells with regard to their response to SM. SM almost exclusively (in our hands) induces necrosis in cultured keratinocytes and only at high concentrations of SM (\geq 500 μ M). However, microfilament disruption, cell rounding and significant loss of keratinocyte adherence were all induced by 250 μ M SM, a concentration of the agent producing little, if any, keratinocyte necrosis. ATP loss was only associated with SM concentrations (\geq 500 μ M) which induced necrosis. Although we were able to see a dose-dependent loss of NAD⁺, we did not observe a

corresponding increase in PARP activity in keratinocytes after SM injury (e.g. figures 10 & 11). Thus, a moderate concentration of SM (250 μ M) is capable of producing the cellular pathology which could support vesication without causing cell lysis. The morphologic and cytoskeletal changes of early apoptosis in SM-injured endothelial cells and the non-apoptotic morphologic and cytoskeletal changes which occur independent of necrosis in SM-injured keratinocytes can support loss of endothelial monolayer integrity and decreased keratinocyte adhesion, respectively, both necessary elements in the vesication process.

In contrast to endothelial cells, there was a measurable loss of GSH in keratinocytes after SM injury (e.g. figures 12 & 13) and this coupled with the presence of S-S crosslinked high molecular weight aggregates on SDS-PAGE run under non-reducing conditions (e.g. fig. 14C & D) is suggestive that SM-injured keratinocytes experience a significant oxidative challenge as part of the injury. This phenomenon in turn may help to determine the necrotic pattern of injury which occurs in SM-injured keratinocytes. The impact of SM on keratinocyte morphology, although different from the endothelial pattern, does lead to some similar outcomes — cell rounding and decreased adherence, both of which could facilitate vesication *in vivo*. Finally, the very different responses of endothelial cells and keratinocytes to SM injury (both key cellular targets in the pathogenesis of vesication), strongly suggests the need to develop multiple therapeutic approaches to prevent or minimize SM-induced vesication.

REFERENCES

1. Vogt, Jr, RF, Dannenberg, Jr, AM, Schofield, BH, Hynes, NA, and Papirmeister, B. Pathogenesis of skin lesions caused by sulfur mustard. *Fundam. Appl. Toxicol.* 4:571-583, 1984.
2. Dannenberg, Jr, AM, Pula, PJ, Liu, LH, Harada, S, Tanaka, F, Vogt, Jr, RF, Kajiki, A, and Higuchi, K. Inflammatory mediators and modulators released in organ culture from rabbit skin lesions produced in vivo by sulfur mustard. *Am. J. Pathol.* 121:15-27, 1985.
3. Petrali, JP, Oglesby, SB and Justus, TA. Morphologic effects of sulfur mustard on a human skin equivalent. *J. Toxicol. - Cut & Ocular Toxicol.* 10:315-324, 1991.
4. Phillips, DR, Jennings, LK, Edwards, HH. Identification of membrane proteins mediating the interaction of human platelets. *J. Cell. Biol.* 86:77-86, 1980.
5. Cassimeris, L, McNeill, H, and Zigmond, SH. Chemoattractant-stimulated polymorphonuclear leukocytes contain two populations of actin filaments that differ in their spatial distributions and relative stabilities. *J. Cell Biol.* 110:1067-1075, 1990.
6. Watts, RG, and Howard, TH. Evidence for a gelsolin-rich, labile F-actin pool in human polymorphonuclear leukocytes. *Cell Motil. Cytoskel.* 21:25-37, 1992.
7. Hinshaw, DB, Burger, JM, Miller, MT, Adams, JA, Beals, TF, and Omann, GM. ATP depletion induces an increase in the assembly of a labile pool of polymerized actin in endothelial cells. *Am. J. Physiol.* 264 (Cell Physiol.33):C1171-C1179, 1993.
8. Schwartzman, RA and Cidlowski, JA. Apoptosis: the biochemistry and molecular biology of programmed cell death. *Endocrine Rev.* 14:133-151, 1993.
9. Schwartz, LM and Osborne, BA. Programmed cell death, apoptosis and killer genes. *Immunol. Today* 14:582-590, 1993.
10. Gerschenson, LE and Rotello, RJ. Apoptosis: a different type of cell death. *FASEB J.* 6:2450-2455, 1992.
11. Papirmeister, B, Feister, AJ, Robinson, SI, and Ford, RD. In *Medical Defense against Mustard Gas: Toxic Mechanisms and Pharmacological Implications*. CRC Press, Inc., Boca Raton, FL, 1991.
12. Papirmeister, B. Does apoptosis (programmed cell death) play a role in sulfur mustard injury? *Medical Chemical Defense* 7:1-12, 1994.
13. Levee, MG, Dabrowska, MI, Lelli, Jr, JL, and Hinshaw, DB. Actin polymerization and depolymerization during apoptosis in HL 60 cells. *Am. J. Physiol.* 271 (Cell Physiol. 40): C1981 - C1992, 1996.
14. Lelli, Jr, JL, Becks, LL, Dabrowska, MI, and Hinshaw, DB. ATP converts necrosis to apoptosis in oxidant-injured endothelial cells. Manuscript to be submitted.
15. Dabrowska, MI, Becks, LL, Lelli, Jr, JL, Levee, MG, and Hinshaw, DB. Sulfur mustard induces apoptosis and necrosis in endothelial cells. *Toxicol. Appl. Pharmacol.* 141: 568-583, 1996.
16. Hockenbery, DM, Oltvai, ZN, Yin, X-M, Millman, CL, and Korsmeyer, SJ. Bcl-2 functions in an antioxidant pathway to prevent apoptosis. *Cell* 75:241-251, 1993.
17. Duke, RC and Cohen, JJ. Morphological and biochemical assays of apoptosis. *Current Protocols in Immunology Suppl.* 3:17:1-16, 1992.
18. Wulf, E, Deboren, A, Bantz, FA, Faulstich, H, and Wieland, TH. Fluorescent phalloxin, a tool for the visualization of cellular actin. *Proc. Natl. Acad. Sci. USA* 76:4498-4502, 1979.

19. Jacobson, EL and Jacobson, MK. Pyridine nucleotide levels as a function of growth in normal and transformed 3T3 cells. *Arch. Biochem. Biophys.* 175:627-634, 1976.
20. Schraufstatter, IU, Hinshaw, DB, Hyslop, PA, Spragg, RG, and Cochrane, CG: Oxidant injury of cells: DNA strand breaks activate poly-ADP-ribose polymerase and lead to depletion of nicotinamide adenine dinucleotide. *J. Clin. Invest.* 77:1312-1320, 1986.
21. Fiskum, G, Craig, SW, Decker, GL, and Lehninger, AL. The cytoskeleton of digitonin-treated rat hepatocytes. *Proc.Natl. Acad. Sci. USA.* 77:3430-3434, 1980.
22. Brehe, JE, and Burch, HB. Enzymatic assay for glutathione. *Anal Biochem.* 74:189, 1976.
23. Griffith, OW. Determination of glutathione and glutathione disulfide using glutathione reductase and 2-vinyl-pyridine. *Anal. Biochem.* 106:207, 1980.
24. Shasby, DM, Lind, SE, Shasby, SS, Goldsmith, JC, and Hunninghake, GW. Reversible oxidant-induced increases in albumin transfer across cultured endothelium: Alterations in cell shape and calcium homeostasis. *Blood.* 65:605, 1985.
25. Nurko, S, Sagabe, K, Davis, JA, Roeser, NF, Defrain, M, Chien, A, Hinshaw, D, Athey, B, Meixner, W, Venkatachalam, MA, and Weinberg, JM. Contribution of actin cytoskeletal alterations to ATP depletion and calcium-induced proximal tubule cell injury. *Am. J. Physiol* 270 (Renal, Fluid Electrolyte, Physiol, 39), F39-F52, 1996.
26. Blikstad, I, Markey, F, Carlsson, L, Persson, T, and Lindberg, U. Selective assay of monomeric and filamentous actin in cell extracts, using inhibition of deoxyribonuclease I. *Cell.* 15:935-943, 1978.
27. Yamamoto, K and Farber, TL. Metabolism of pyridine nucleotides in cultured rat hepatocytes intoxicated with tert-Butyl Hydroperoxide. *Biochem. Pharmacol.* 43:1119-1126, 1992.
28. Carson, DA, Seto, S, Wasson, DB, and Carrera, CT. DNA strand breaks, NAD metabolism, and programmed cell death. *Exp. Cell Res.* 164: 273-281, 1986.
29. McCreanor, GM and Bender, DA. The role of catabolism in controlling tissue concentrations of nicotinamide nucleotide coenzymes. *Biochem. Biophys. Acta* 759:222-228, 1983.
30. Hinshaw, DB, Sklar, L, Bohl, B, Schraufstatter, I, Hyslop, P, Rossi, M, Spragg, R and Cochrane, CG. Cytoskeletal and morphological impact of cellular oxidant injury. *Am. J. Pathol.* 123:454-464, 1986.

BIBLIOGRAPHY

Abstracts/Presentations:

1. Levee, MG, Dabrowska, MI, Lelli, Jr, JL, and Hinshaw, DB. Actin depolymerization is a consistent feature of apoptosis in HL-60 cells. FASEB J. 10: A63, 1996.
2. Lelli, JR. JL, Becks, LL, Dabrowska, MI, and Hinshaw, DB. ATP converts necrosis to apoptosis in oxidant-injured endothelial cells. Oral presentation at Oxygen Society (November 1996).
3. Immunopathology Symposium in honor of Charles G. Cochrane, M.D., La Jolla, CA. "Microfilament pathology induced by oxidants or ischemic conditions." October 14, 1995.
4. Medical Defense Bioscience Review, Department of Defense, Baltimore, MD. "Sulfur Mustard Induces Apoptosis and Necrosis in Endothelial Cells." May 15, 1996.

Publications:

1. Levee, MG, Dabrowska, MI, Lelli, Jr, JL, and Hinshaw, DB. Actin polymerization and depolymerization during apoptosis in HL 60 cells. Am. J. Physiol. 271 (Cell Physiol. 40): C1981-C1992, 1996.
2. Dabrowska, MI, Becks, LL, Lelli, Jr, JL, Levee, MG, and Hinshaw, DB. Sulfur mustard induces apoptosis and necrosis in endothelial cells. Toxicol. Appl. Pharmacol. 141: 568-583, 1996.

Manuscripts in preparation *:

1. Lelli, Jr, JL, Becks, LL, Dabrowska, MI, and Hinshaw, DB. ATP converts necrosis to apoptosis in oxidant-injured endothelial cells.

* To be submitted in a few weeks, at which time we will also forward a copy for internal DOD review.

PERSONNEL (receiving support from MIPR 93MM3571):

Jeanne Burger, B.S.	7/1/93-6/20/95	full time
Minette Levee, M.S.	1/31/94-6/7/96	part time
Milena Dabrowska, Ph.D.	4/2/95-8/16/96	full time